Journal of Systems Engineering and Electronics
Vol. 32, No. 5, October 2021, pp.995 – 1013

Unified control and detection framework and its applications: a review, some new results, and future perspectives

DING Steven Xianchuan[1], LI Linlin[2,*], and JIANG Bin[3]

1. Institute for Automatic Control and Complex Systems, University of Duisburg-Essen, Duisburg 47057, Germany;
2. School of Automation and Electrical Engineering, University of Science and Technology Beijing, Beijing 100083, China;
3. College of Automation Engineering, Nanjing University of Aeronautics and Astronautics, Nanjing 210016, China

Abstract: Initiated three decades ago, integrated design of controllers and fault detectors has continuously attracted research attention. The recent development of the unified control and detection framework with an observer-based residual generator in its core gives a more general form of the previous works. Its applications to residual centred modelling of uncertain control systems, fault detection in feedback control systems with uncertainties, fault-tolerant control (FTC) as well as control performance degradation monitoring, detection and recovery are introduced. In conclusion, some future perspectives are proposed.

Keywords: unified framework of control and detection, observer-based residual generator, Youla parameterisation, detection of additive and multiplicative faults in control loop, fault-tolerant control (FTC), loop performance degradation (LPD) monitoring and recovery.

DOI: 10.23919/JSEE.2021.000085

1. Introduction

It is state of the art that fault detection and isolation (FDI) functional units are, in parallel to control functional units, widely integrated into new generation of automatic control systems, in particular when the control systems are integrated into safety relevant processes, for instance, transport and vehicles systems, and aircraft and chemical plants [1−3]. The diagnostic algorithms are often constructed separately from the control ones, although both the control and diagnostic functional modules are designed based on an identical system model [1]. A critical issue of integrating a diagnostic module into a feedback control loop is the interactions between control and diagnosis. Having noticed the importance of this issue three decades ago, Nett et al. initiated the study on the integrated design of control and diagnosis [4], which received much attention in the 1990s [5−10]. The original idea of the integrated design scheme proposed by Nett et al. was to manage the interactions between the control and diagnostic algorithms in an integrated manner [5]. To this end, system configuration with an integrated control and diagnostic module was proposed. In this way, design of the control and diagnostic units is considered as a standard feedback control problem [8−10], and the potential interactions between them can be systematically addressed in the so-called $\mathcal{H}_\infty$ optimisation framework that was very popular at that time and well established in the robust control theory [11]. These methods have been further improved and extended in the next decade [12−14]. The research efforts and the achieved results in these two decades were reviewed in [15].

Parallel to the above investigations, alternative schemes towards integrated design and configuration of control and detection functionalities have been reported, which can be classified into three groups: (i) integration of the residual generator that runs in parallel to the controller, as proposed in [16]; (ii) application of the standard observer-based control scheme with the observer-based controller delivering both the control and diagnostic signals, as proposed in [17]; (iii) implementing the Youla parameterisation controllers [11] in the residual generator form, the so-called generalised internal model control [18] structure (GIMC).

Inspired by the investigation in [18], Ding et al. proposed an observer-based parameterisation of all stabilising controllers with an observer-based residual generator in its core and demonstrated its successful application to control and detection of engine management systems [19]. On the basis of this work, a new unified framework of control and detection has been recently established. This framework generalises the integrated design methods

Manuscript received February 01, 2021.
*Corresponding author.
This work was supported by the National Natural Science Foundation of China (62020106003, 62073029), the Beijing Natural Science Foundation (4202045), and the Fundamental Research Funds for the Central Universities (FRF-TP-20-012A3).

of control and detection developed in the past decades and has been applied to dealing with issues like fault diagnosis in automatic control systems with uncertainties, fault-tolerant control (FTC) and, more recently, to control performance degradation detection and recovery. The major objective of this paper is to report the results achieved in this context. In the first part of this paper, a review is dedicated to an introduction of the basics of the integrated control and detection framework. It is not a typical literature survey. The main part includes a detailed summary of the recent results of applying the unified control and detection framework to fault detection, performance degradation monitoring and recovering. The last part is devoted to some promising future perspectives in the context of the framework.

This paper is organised as follows. In Section 2, the unified framework of control and detection, together with the necessary control theoretical and mathematical preliminaries, is first presented. Section 3 is dedicated to the introduction and review of some methodical applications of the unified framework, including (i) residual centred modelling of uncertain control systems, (ii) fault detection in control systems with uncertainties, (iii) FTC, and (iv) control performance degradation detection and recovery. The future perspectives of the unified framework are shortly summarised in Section 4.

Throughout this paper, standard notation known in linear algebra and the advanced control theory is adopted. In addition, notation $\mathcal{RH}_\infty$ is adopted for presenting the set of all stable systems.

2. Review of the unified control and detection framework

The unified control and detection framework is established on the basis of the so-called system factorisation technique and the well-known Youla parameterisation of all stabilising controllers.

2.1 System representations

2.1.1 System factorisations and their interpretations

Consider a linear time-invariant (LTI) system modelled by

$$\boldsymbol{y}(z)=\boldsymbol{G}(z)\boldsymbol{u}(z) \tag{1}$$

with $\boldsymbol{u}\in\mathbf{R}^p$ and $\boldsymbol{y}\in\mathbf{R}^m$ as the plant input and output vectors. Suppose that $\boldsymbol{G}(z)$ is a proper real-rational matrix with the minimal state space realisation

$$\boldsymbol{x}(k+1)=\boldsymbol{A}\boldsymbol{x}(k)+\boldsymbol{B}\boldsymbol{u}(k),\ \ \boldsymbol{x}(0)=\boldsymbol{x}_0, \tag{2}$$

$$\boldsymbol{y}(k)=\boldsymbol{C}\boldsymbol{x}(k)+\boldsymbol{D}\boldsymbol{u}(k), \tag{3}$$

where $\boldsymbol{x}\in\mathbf{R}^n$ is the state vector and matrices $\boldsymbol{A},\boldsymbol{B},\boldsymbol{C},\boldsymbol{D}$ are real constant matrices of appropriate dimensions. A coprime factorisation of $\boldsymbol{G}(z)$ over $\mathcal{RH}_\infty$ factorises $\boldsymbol{G}(z)$ into two stable and coprime transfer matrices. They are called left and right coprime factorisations (LCF and RCF) and given by

$$\boldsymbol{G}(z)=\hat{\boldsymbol{M}}^{-1}(z)\hat{\boldsymbol{N}}(z)=\boldsymbol{N}(z)\boldsymbol{M}^{-1}(z) \tag{4}$$

where $\left(\hat{\boldsymbol{M}}(z),\hat{\boldsymbol{N}}(z)\right)$ and $(\boldsymbol{M}(z),\boldsymbol{N}(z))$ are the left and right coprime pairs (LCP and RCP) of $\boldsymbol{G}(z)$. Correspondingly, there exist RCP and LCP $\left(\hat{\boldsymbol{X}}(z),\hat{\boldsymbol{Y}}(z)\right)$ and $(\boldsymbol{X}(z),\boldsymbol{Y}(z))$ so that the well-known Bezout identity holds [11]

$$\begin{bmatrix}\boldsymbol{X}(z) & \boldsymbol{Y}(z)\\ -\hat{\boldsymbol{N}}(z) & \hat{\boldsymbol{M}}(z)\end{bmatrix}\begin{bmatrix}\boldsymbol{M}(z) & -\hat{\boldsymbol{Y}}(z)\\ \boldsymbol{N}(z) & \hat{\boldsymbol{X}}(z)\end{bmatrix}=\begin{bmatrix}\boldsymbol{I} & \boldsymbol{0}\\ \boldsymbol{0} & \boldsymbol{I}\end{bmatrix}. \tag{5}$$

The state space realisations of these eight transfer function matrices are

$$\begin{cases}\hat{\boldsymbol{M}}(z)=(\boldsymbol{A}-\boldsymbol{L}\boldsymbol{C},-\boldsymbol{L},\boldsymbol{C},\boldsymbol{I})\\ \hat{\boldsymbol{N}}(z)=(\boldsymbol{A}-\boldsymbol{L}\boldsymbol{C},\boldsymbol{B}-\boldsymbol{L}\boldsymbol{D},\boldsymbol{C},\boldsymbol{D})\end{cases}, \tag{6}$$

$$\begin{cases}\boldsymbol{M}(z)=(\boldsymbol{A}+\boldsymbol{B}\boldsymbol{F},\boldsymbol{B},\boldsymbol{F},\boldsymbol{I})\\ \boldsymbol{N}(z)=(\boldsymbol{A}+\boldsymbol{B}\boldsymbol{F},\boldsymbol{B},\boldsymbol{C}+\boldsymbol{D}\boldsymbol{F},\boldsymbol{D})\end{cases}, \tag{7}$$

$$\begin{cases}\hat{\boldsymbol{X}}(z)=(\boldsymbol{A}+\boldsymbol{B}\boldsymbol{F},\boldsymbol{L},\boldsymbol{C}+\boldsymbol{D}\boldsymbol{F},\boldsymbol{I})\\ \hat{\boldsymbol{Y}}(z)=(\boldsymbol{A}+\boldsymbol{B}\boldsymbol{F},-\boldsymbol{L},\boldsymbol{F},\boldsymbol{0})\end{cases}, \tag{8}$$

$$\begin{cases}\boldsymbol{X}(z)=(\boldsymbol{A}-\boldsymbol{L}\boldsymbol{C},-(\boldsymbol{B}-\boldsymbol{L}\boldsymbol{D}),\boldsymbol{F},\boldsymbol{I})\\ \boldsymbol{Y}(z)=(\boldsymbol{A}-\boldsymbol{L}\boldsymbol{C},-\boldsymbol{L},\boldsymbol{F},\boldsymbol{0})\end{cases}, \tag{9}$$

which can be interpreted, with different input and output variables [20], as follows:

(i) a (full) state observer and observer-based residual generator,

$$\hat{\boldsymbol{x}}(k+1)=\boldsymbol{A}\hat{\boldsymbol{x}}(k)+\boldsymbol{B}\boldsymbol{u}(k)+\boldsymbol{L}(\boldsymbol{y}(k)-\hat{\boldsymbol{y}}(k)), \tag{10}$$

$$\boldsymbol{r}_0(k)=\boldsymbol{y}(k)-\hat{\boldsymbol{y}}(k),\hat{\boldsymbol{y}}(k)=\boldsymbol{C}\hat{\boldsymbol{x}}(k)+\boldsymbol{D}\boldsymbol{u}(k) \tag{11}$$

$\Longleftrightarrow$

$$\boldsymbol{r}_0(z)=\hat{\boldsymbol{M}}(z)\boldsymbol{y}(z)-\hat{\boldsymbol{N}}(z)\boldsymbol{u}(z), \tag{12}$$

(ii) an observer-based state feedback controller and its input-output dynamics,

$$\hat{\boldsymbol{x}}(k+1)=(\boldsymbol{A}+\boldsymbol{B}\boldsymbol{F})\hat{\boldsymbol{x}}(k)+\boldsymbol{L}\boldsymbol{r}_0(k), \tag{13}$$

$$\begin{bmatrix}\boldsymbol{u}(k)\\ \boldsymbol{y}(k)\end{bmatrix}=\begin{bmatrix}\boldsymbol{0}\\ \boldsymbol{I}\end{bmatrix}\boldsymbol{r}_0(k)+\begin{bmatrix}\boldsymbol{F}\\ \boldsymbol{C}+\boldsymbol{D}\boldsymbol{F}\end{bmatrix}\hat{\boldsymbol{x}}(k) \tag{14}$$

$\Longleftrightarrow$

$$\begin{bmatrix}\boldsymbol{u}(z)\\ \boldsymbol{y}(z)\end{bmatrix}=\begin{bmatrix}-\hat{\boldsymbol{Y}}(z)\\ \hat{\boldsymbol{X}}(z)\end{bmatrix}\boldsymbol{r}_0(z), \tag{15}$$

(iii) a state feedback controller and its input-output dynamics,

$$\boldsymbol{x}(k+1)=(\boldsymbol{A}+\boldsymbol{B}\boldsymbol{F})\boldsymbol{x}(k)+\boldsymbol{B}\boldsymbol{v}(k), \tag{16}$$

$$\begin{bmatrix}\boldsymbol{u}(k)\\ \boldsymbol{y}(k)\end{bmatrix}=\begin{bmatrix}\boldsymbol{F}\\ \boldsymbol{C}+\boldsymbol{D}\boldsymbol{F}\end{bmatrix}\boldsymbol{x}(k)+\begin{bmatrix}\boldsymbol{I}\\ \boldsymbol{D}\end{bmatrix}\boldsymbol{v}(k) \tag{17}$$

$\Longleftrightarrow$

$$\begin{bmatrix} \boldsymbol{u}(z) \\ \boldsymbol{y}(z) \end{bmatrix} = \begin{bmatrix} \boldsymbol{M}(z) \\ \boldsymbol{N}(z) \end{bmatrix} \boldsymbol{v}(z), \tag{18}$$

(iv) an observer-based state feedback controller and the closed-loop "residual generator"

$$\hat{\boldsymbol{x}}(k+1) = (\boldsymbol{A} - \boldsymbol{LC})\hat{\boldsymbol{x}}(k) + (\boldsymbol{B} - \boldsymbol{LD})\boldsymbol{u}(k) + \boldsymbol{L}\boldsymbol{y}(k), \tag{19}$$

$$\boldsymbol{v}(k) = \boldsymbol{u}(k) - \boldsymbol{F}\hat{\boldsymbol{x}}(k) \tag{20}$$

$\Longleftrightarrow$

$$\boldsymbol{v}(z) = \boldsymbol{X}(z)\boldsymbol{u}(z) + \boldsymbol{Y}(z)\boldsymbol{y}(z). \tag{21}$$

In (10)−(12), the LCP $\left(\hat{\boldsymbol{M}}, \hat{\boldsymbol{N}}\right)$ is an observer-based residual generator for a plant $\boldsymbol{G}$ with $(\boldsymbol{u}, \boldsymbol{y})$ as its input variables and the primary residual $\boldsymbol{r}_0$ as the output. Systems (13)−(15) can be understood as an observer-based state feedback control loop driven by the (primary) residual $\boldsymbol{r}_0$ and delivers $(\boldsymbol{u}, \boldsymbol{y})$. In this sense, $\left(\hat{\boldsymbol{X}}, \hat{\boldsymbol{Y}}\right)$ is an RCP of an observer-based controller. Systems $(\boldsymbol{M}, \boldsymbol{N})$ and $(\boldsymbol{X}, \boldsymbol{Y})$ given in (16)−(21) are in fact the dual forms of $\left(\hat{\boldsymbol{M}}, \hat{\boldsymbol{N}}\right)$ and $\left(\hat{\boldsymbol{X}}, \hat{\boldsymbol{Y}}\right)$, respectively. While $(\boldsymbol{M}, \boldsymbol{N})$ is a state feedback control loop with the reference signal $\boldsymbol{v}$ as its input and $(\boldsymbol{u}, \boldsymbol{y})$ as the (loop) output vector, $(\boldsymbol{X}, \boldsymbol{Y})$ represents an observer-based closed-loop dynamics driven by the plant input and output, $(\boldsymbol{u}, \boldsymbol{y})$, and, based on it, the "residual signal" $\boldsymbol{v}$ is generated. It forms in fact an LCP of the observer-based state feedback controller. In the context of the above-described interpretations, matrices $\boldsymbol{F}$ and $\boldsymbol{L}$ are often called state feedback gain and observer gain matrices and are to be selected such that $\boldsymbol{A} + \boldsymbol{BF}$ and $\boldsymbol{A} - \boldsymbol{LC}$ are Schur [20].

Corresponding to the LCF and RCF, there exist further two equivalent model forms, the so-called stable kernel and image representations (SKR and SIR), for a given system. For instance, given system $\boldsymbol{y}(z) = \boldsymbol{G}(z)\boldsymbol{u}(z)$, its SKR and SIR are respectively described by

$$\text{SKR}: \boldsymbol{r}_0(z) = \hat{\boldsymbol{M}}(z)\boldsymbol{y}(z) - \hat{\boldsymbol{N}}(z)\boldsymbol{u}(z), \tag{22}$$

$$\text{SIR}: \begin{bmatrix} \boldsymbol{u}(z) \\ \boldsymbol{y}(z) \end{bmatrix} = \begin{bmatrix} \boldsymbol{M}(z) \\ \boldsymbol{N}(z) \end{bmatrix} \boldsymbol{v}(z). \tag{23}$$

Note that when $\hat{\boldsymbol{x}}(0) = \boldsymbol{x}(0)$, it holds

$$\boldsymbol{r}_0(z) = \hat{\boldsymbol{M}}(z)\boldsymbol{y}(z) - \hat{\boldsymbol{N}}(z)\boldsymbol{u}(z) = \boldsymbol{0}$$

$\Longleftrightarrow$

$$\boldsymbol{y}(z) = \hat{\boldsymbol{M}}^{-1}(z)\hat{\boldsymbol{N}}(z)\boldsymbol{u}(z) = \boldsymbol{G}(z)\boldsymbol{u}(z).$$

Moreover, it follows from (23) that

$$\boldsymbol{y}(z) = \boldsymbol{N}(z)\boldsymbol{v}(z) = \boldsymbol{N}(z)\boldsymbol{M}^{-1}(z)\boldsymbol{u}(z) = \boldsymbol{G}(z)\boldsymbol{u}(z).$$

2.1.2 Modelling of nominal system dynamics, uncertainties and faults

When a control system is operating under the fault- and uncertainty-free condition, its dynamics is called nominal and denoted, in the sequel, by

$$\boldsymbol{y}(z) = \boldsymbol{G}_0(z)\boldsymbol{u}(z) \tag{24}$$

with (2) and (3) as its minimal state space realisation. Correspondingly, the LCP and RCP of $\boldsymbol{G}_0$ are denoted by $\left(\hat{\boldsymbol{M}}_0, \hat{\boldsymbol{N}}_0\right)$ and $(\boldsymbol{M}_0, \boldsymbol{N}_0)$. And associated with them, we have $\left(\hat{\boldsymbol{X}}_0, \hat{\boldsymbol{Y}}_0\right)$ and $(\boldsymbol{X}_0, \boldsymbol{Y}_0)$.

Extending (2) and (3) to

$$\boldsymbol{x}(k+1) = \boldsymbol{A}\boldsymbol{x}(k) + \boldsymbol{B}\boldsymbol{u}(k) + \boldsymbol{E}_d\boldsymbol{d}(k), \tag{25}$$

$$\boldsymbol{y}(k) = \boldsymbol{C}\boldsymbol{x}(k) + \boldsymbol{D}\boldsymbol{u}(k) + \boldsymbol{F}_d\boldsymbol{d}(k) \tag{26}$$

leads to

$$\boldsymbol{y}(z) = \boldsymbol{G}_0(z)\boldsymbol{u}(z) + \boldsymbol{G}_d(z)\boldsymbol{d}(z), \tag{27}$$

$$\boldsymbol{G}_d(z) = \boldsymbol{F}_d + \boldsymbol{C}(z\boldsymbol{I} - \boldsymbol{A})^{-1}\boldsymbol{E}_d, \tag{28}$$

where $\boldsymbol{d}(k) \in \mathbf{R}^{k_d}$ is an unknown input vector, $\boldsymbol{E}_d$ and $\boldsymbol{F}_d$ are known and of appropriate dimensions. $\boldsymbol{d}$ can represent either the (additive) fault vector (in the literature, notation $\boldsymbol{f}(k)$ is often adopted) or the disturbance vector. Although many research works are focused on additive faults and unknown disturbances, their influences on the control system performance are minor critical, since they do not affect the system stability and eigen-dynamics. Moreover, there exist rich well-developed methods to detect and further to compensate and minimise their influences. Differently, uncertainties or/and faults caused by changes in the system parameters could be more critical. For instance, unknown variations modelled by $\boldsymbol{\Delta}_A, \boldsymbol{\Delta}_B, \boldsymbol{\Delta}_C$, and $\boldsymbol{\Delta}_D$ in the system representation,

$$\boldsymbol{x}(k+1) = (\boldsymbol{A} + \boldsymbol{\Delta}_A)\boldsymbol{x}(k) + (\boldsymbol{B} + \boldsymbol{\Delta}_B)\boldsymbol{u}(k), \tag{29}$$

$$\boldsymbol{y}(k) = (\boldsymbol{C} + \boldsymbol{\Delta}_C)\boldsymbol{x}(k) + (\boldsymbol{D} + \boldsymbol{\Delta}_D)\boldsymbol{u}(k), \tag{30}$$

could remarkably change the system dynamics. Typically, such change is a slowly varying process, beginning as minor parameter variations and thus treated as tolerable model uncertainties. With increasing time, they could become severe faults and considerably affect the system performance. Hence, an early detection of this class of faults, addressed in the literature as detection of incipient faults, and subsequent online updating of the control system are of considerable practical interests, but considerably challenging for research work. In our subsequent study, we will not distinguish between parameter uncertainties and faults, which are also called multiplicative faults, by notation, and call them uniformly uncertainties, when there is no risk of confusion. Let $\boldsymbol{G}(z)$ be the transfer function of the uncertain system (29)−(30), and

$$\begin{cases} \hat{\boldsymbol{M}}(z) = (\boldsymbol{A}_\Delta - \boldsymbol{L}\boldsymbol{C}_\Delta, -\boldsymbol{L}, \boldsymbol{C}_\Delta, \boldsymbol{I}) \\ \hat{\boldsymbol{N}}(z) = (\boldsymbol{A}_\Delta - \boldsymbol{L}\boldsymbol{C}_\Delta, \boldsymbol{B}_\Delta - \boldsymbol{L}\boldsymbol{D}_\Delta, \boldsymbol{C}_\Delta, \boldsymbol{D}_\Delta) \end{cases}, \tag{31}$$

$$\begin{cases} \boldsymbol{M}(z) = (\boldsymbol{A}_\Delta + \boldsymbol{B}_\Delta\boldsymbol{F}, \boldsymbol{B}_\Delta, \boldsymbol{F}, \boldsymbol{I}) \\ \boldsymbol{N}(z) = (\boldsymbol{A}_\Delta + \boldsymbol{B}_\Delta\boldsymbol{F}, \boldsymbol{B}_\Delta, \boldsymbol{C}_\Delta + \boldsymbol{D}_\Delta\boldsymbol{F}, \boldsymbol{D}_\Delta) \end{cases}, \tag{32}$$

$$\begin{cases} \boldsymbol{A}_\Delta = \boldsymbol{A} + \boldsymbol{\Delta}_A \\ \boldsymbol{B}_\Delta = \boldsymbol{B} + \boldsymbol{\Delta}_B \\ \boldsymbol{C}_\Delta = \boldsymbol{C} + \boldsymbol{\Delta}_C \\ \boldsymbol{D}_\Delta = \boldsymbol{D} + \boldsymbol{\Delta}_D \end{cases}, \tag{33}$$

be its LCP and RCP, i.e.,

$$\boldsymbol{y}(z) = \boldsymbol{G}(z)\boldsymbol{u}(z) = \hat{\boldsymbol{M}}^{-1}(z)\hat{\boldsymbol{N}}(z)\boldsymbol{u}(z) = \boldsymbol{N}(z)\boldsymbol{M}^{-1}(z)\boldsymbol{u}(z). \tag{34}$$

Define

$$\begin{cases} \boldsymbol{\Delta}_{\hat{M}} = \hat{\boldsymbol{M}}(z) - \hat{\boldsymbol{M}}_0(z) \\ \boldsymbol{\Delta}_{\hat{N}} = \hat{\boldsymbol{N}}(z) - \hat{\boldsymbol{N}}_0(z) \end{cases}, \tag{35}$$

$$\begin{cases} \boldsymbol{\Delta}_M = \boldsymbol{M}(z) - \boldsymbol{M}_0(z) \\ \boldsymbol{\Delta}_N = \boldsymbol{N}(z) - \boldsymbol{N}_0(z) \end{cases}. \tag{36}$$

The uncertain system (34) can be written as

$$\boldsymbol{y}(z) = \left(\hat{\boldsymbol{M}}_0(z) + \boldsymbol{\Delta}_{\hat{M}}\right)^{-1}\left(\hat{\boldsymbol{N}}_0(z) + \boldsymbol{\Delta}_{\hat{N}}\right)\boldsymbol{u}(z) = \tag{37}$$

$$(\boldsymbol{N}_0(z) + \boldsymbol{\Delta}_N)(\boldsymbol{M}_0(z) + \boldsymbol{\Delta}_M)^{-1}\boldsymbol{u}(z). \tag{38}$$

In our work, it is assumed, without loss of generality [21], that systems with uncertainties are modelled by (37) or (38) and call

$$\begin{bmatrix} \boldsymbol{\Delta}_{\hat{N}} & \boldsymbol{\Delta}_{\hat{M}} \end{bmatrix} \in \mathcal{RH}_\infty, \begin{bmatrix} \boldsymbol{\Delta}_N \\ \boldsymbol{\Delta}_M \end{bmatrix} \in \mathcal{RH}_\infty$$

left and right coprime factor uncertainties (LCFU and RCFU). Moreover, both the unknown input vector, LCFU and RCFU are norm-bounded as

$$\|\boldsymbol{d}\|_2 \leqslant \delta_d, \left\|\begin{bmatrix} \boldsymbol{\Delta}_{\hat{N}} & \boldsymbol{\Delta}_{\hat{M}} \end{bmatrix}\right\|_\infty \leqslant \delta_{\mathcal{K}}, \left\|\begin{bmatrix} \boldsymbol{\Delta}_N \\ \boldsymbol{\Delta}_M \end{bmatrix}\right\|_\infty \leqslant \delta_{\mathcal{I}}.$$

2.2 Youla parameterisation of stabilising controllers

The feedback control loops under consideration are sketched in Fig. 1 with the plant model $\boldsymbol{G}(z)$ and controller

$$\boldsymbol{u}(z) = \boldsymbol{K}(z)\boldsymbol{y}(z) + \boldsymbol{v}(z) \tag{39}$$

where $\boldsymbol{v}(z)$ is the reference signal. Given the LCP and RCP of the nominal plant model $\boldsymbol{G}_0, \left(\hat{\boldsymbol{M}}_0, \hat{\boldsymbol{N}}_0\right)$, $(\boldsymbol{M}_0, \boldsymbol{N}_0)$, as well as the associated RCP and LCP $\left(\hat{\boldsymbol{X}}_0, \hat{\boldsymbol{Y}}_0\right)$ and $(\boldsymbol{X}_0, \boldsymbol{Y}_0)$ satisfying Bezout identity (5), it is a well-known result that all stabilising controllers can be parameterised by

$$\boldsymbol{K}(z) = -\left(\boldsymbol{X}_0(z) - \boldsymbol{Q}(z)\hat{\boldsymbol{N}}_0(z)\right)^{-1}\left(\boldsymbol{Y}_0(z) + \boldsymbol{Q}(z)\hat{\boldsymbol{M}}_0(z)\right) \tag{40}$$

$$\boldsymbol{K}(z) = -\left(\hat{\boldsymbol{Y}}_0(z) + \boldsymbol{M}_0(z)\boldsymbol{Q}(z)\right)\left(\hat{\boldsymbol{X}}_0(z) - \boldsymbol{N}_0(z)\boldsymbol{Q}(z)\right)^{-1} \tag{41}$$

with parameter system $\boldsymbol{Q}(z) \in \mathcal{RH}_\infty$. The parameterisation expression (40)−(41) is called Youla parameterisation [11].

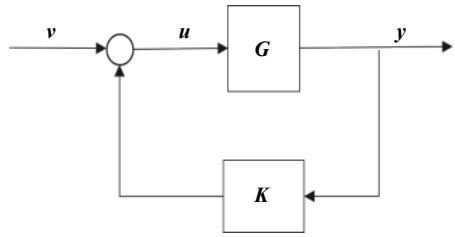

Fig. 1 Feedback control loop under consideration

2.3 Basics of the unified framework of control and detection

We are now in the position to review the basics of the control and detection unified framework.

2.3.1 Observer-based realisation of Youla parameterisation

It follows from (6), (9), and (40), as well as Bezout identity (5) that any (stabilising) output feedback controller described by (39) can be equivalently written as

$$\hat{\boldsymbol{x}}(k+1) = \boldsymbol{A}\hat{\boldsymbol{x}}(k) + \boldsymbol{B}\boldsymbol{u}(k) + \boldsymbol{L}\boldsymbol{r}_0(k), \tag{42}$$

$$\begin{cases} \boldsymbol{r}_0(k) = \boldsymbol{y}(k) - \hat{\boldsymbol{y}}(k) \\ \hat{\boldsymbol{y}}(k) = \boldsymbol{C}\hat{\boldsymbol{x}}(k) + \boldsymbol{D}\boldsymbol{u}(k) \end{cases}, \tag{43}$$

$$\begin{cases} \boldsymbol{u}(z) = \boldsymbol{F}\hat{\boldsymbol{x}}(z) - \boldsymbol{Q}(z)\boldsymbol{r}_0(z) + \bar{\boldsymbol{v}}(z) \\ \bar{\boldsymbol{v}}(z) = \left(\boldsymbol{X}_0(z) - \boldsymbol{Q}(z)\hat{\boldsymbol{N}}_0(z)\right)\boldsymbol{v}(z) \end{cases}. \tag{44}$$

That means, any dynamic output feedback controller is an observer-based controller and driven by the residual signal $\boldsymbol{r}_0$. In fact, a special case of this realisation, $\boldsymbol{Q}(z) = 0$, has been demonstrated by (15) in the context of interpreting the RCP $\left(\hat{\boldsymbol{X}}_0, \hat{\boldsymbol{Y}}_0\right)$ of the controller. Note that the state space representation (42)−(44) can also be written as

$$\begin{bmatrix} \boldsymbol{u}(z) \\ \boldsymbol{y}(z) \end{bmatrix} = \begin{bmatrix} -\hat{\boldsymbol{Y}}_0(z) - \boldsymbol{M}_0(z)\boldsymbol{Q}(z) \\ \hat{\boldsymbol{X}}_0(z) - \boldsymbol{N}_0(z)\boldsymbol{Q}(z) \end{bmatrix}\boldsymbol{r}_0(z) + \begin{bmatrix} \boldsymbol{M}_0(z) \\ \boldsymbol{N}_0(z) \end{bmatrix}\bar{\boldsymbol{v}}(z) = \begin{bmatrix} -\hat{\boldsymbol{Y}}_0(z) - \boldsymbol{M}_0(z)\boldsymbol{Q}(z) \\ \hat{\boldsymbol{X}}_0(z) - \boldsymbol{N}_0(z)\boldsymbol{Q}(z) \end{bmatrix}\boldsymbol{r}_0(z) + \begin{bmatrix} \boldsymbol{I} - \left(\boldsymbol{M}_0(z)\boldsymbol{Q}(z) + \hat{\boldsymbol{Y}}_0(z)\right)\hat{\boldsymbol{N}}_0(z) \\ \left(\hat{\boldsymbol{X}}_0(z) - \boldsymbol{N}_0(z)\boldsymbol{Q}(z)\right)\hat{\boldsymbol{N}}_0(z) \end{bmatrix}\boldsymbol{v}(z)$$

$$\Longleftrightarrow$$

$$\begin{bmatrix} \boldsymbol{u}(z) - \boldsymbol{v}(z) \\ \boldsymbol{y}(z) \end{bmatrix} = \begin{bmatrix} -\hat{\boldsymbol{Y}}_0(z) - \boldsymbol{M}_0(z)\boldsymbol{Q}(z) \\ \hat{\boldsymbol{X}}_0(z) - \boldsymbol{N}_0(z)\boldsymbol{Q}(z) \end{bmatrix}\left(\boldsymbol{r}_0(z) + \hat{\boldsymbol{N}}_0(z)\boldsymbol{v}(z)\right).$$

It follows from (42)−(44) that both controller and detector are driven by the residual signal and thus integratedly constructed on a common observer-based residual generator. Moreover, the observer parameterisation [1] reveals a deeper insight into the information aspect of a feedback controller: the control signal in (44) is an estimate for $\boldsymbol{F}\boldsymbol{x}(k)+\bar{\boldsymbol{v}}(k)$ and satisfies

$$\forall \boldsymbol{x}(0),\boldsymbol{u}(k),\quad \lim_{k\to\infty}(\boldsymbol{u}(k)-\boldsymbol{F}\boldsymbol{x}(k)-\bar{\boldsymbol{v}}(k))=0, \tag{45}$$

when there exists no uncertainty in the plant. The observer-based controller realisation (42)−(44) and the estimator interpretation of output feedback controllers are the core of the unified control and detection framework and the basis of our subsequent study.

2.3.2 Functionalisation of controllers

The configuration of an observer-based stabilising controller (42)−(44) consists of several functional modules:

(i) An observer and an observer-based residual generator as an information provider for the controller and diagnostic system,

$$\begin{aligned}\hat{\boldsymbol{x}}(k+1)&=\boldsymbol{A}\hat{\boldsymbol{x}}(k)+\boldsymbol{B}\boldsymbol{u}(k)+\boldsymbol{L}\boldsymbol{r}_0(k),\\ \boldsymbol{r}_0(k)&=\boldsymbol{y}(k)-\hat{\boldsymbol{y}}(k),\\ \hat{\boldsymbol{y}}(k)&=\boldsymbol{C}\hat{\boldsymbol{x}}(k)+\boldsymbol{D}\boldsymbol{u}(k).\end{aligned}$$

They deliver state estimate $\hat{\boldsymbol{x}}$, and the primary residual, $\boldsymbol{r}_0=\boldsymbol{y}-\hat{\boldsymbol{y}}$.

(ii) Two controllers $\boldsymbol{u}(z)=\boldsymbol{F}\hat{\boldsymbol{x}}(z)-\boldsymbol{Q}(z)\boldsymbol{r}_0(z)+\bar{\boldsymbol{v}}(z)$, $-\boldsymbol{F}\hat{\boldsymbol{x}}(z)-\boldsymbol{Q}(z)\boldsymbol{r}_0(z)$ as feedback controllers, and $-\bar{\boldsymbol{v}}(z)=\boldsymbol{V}(z)\boldsymbol{v}(z),\boldsymbol{V}(z)=\boldsymbol{X}_0(z)-\boldsymbol{Q}(z)\hat{\boldsymbol{N}}_0(z)$ as feed-forward controllers.

(iii) A detector $\boldsymbol{R}(z)\boldsymbol{r}_0(z)$ can be integrated for the detection purpose with $\boldsymbol{R}(z)$ as a (stable) post-filter.

This modular configuration allows a clear parameterisation of the embedded functional modules: $\boldsymbol{L}$ for parameterising the state observer, $\boldsymbol{F}$ and $\boldsymbol{Q}(z)$ for the feedback controller, $\boldsymbol{V}(z)$ for the feed-forward controller, and $\boldsymbol{R}(z)$ for the detector.

It is evident that all the above five parameters have evidently different functionalities. They are summarised as follows: $\boldsymbol{F}$ and $\boldsymbol{L}$ for determining the closed-loop stability and eigen-dynamics; $\boldsymbol{Q}(z)$ for enhancing the system robustness and control performance; $\boldsymbol{R}(z)$ serving for optimising the fault detectability; $\boldsymbol{V}(z)$ for the tracking behaviour.

Due to their different functionalities, these parameters should be treated with different priorities. The fundamental importance of the system stability and eigen-dynamics requires the highest priority of tuning of $\boldsymbol{F}$ and $\boldsymbol{L}$. When a temporary system performance degradation is tolerable, the priority for an online optimisation of $\boldsymbol{Q},\boldsymbol{R}$, and $\boldsymbol{V}$ is lower.

2.3.3 Variations of Youla parameterisation

An immediate application of the observer-based realisation of (42)−(44) and controller functionalisation is the establishment of the so-called FTC system architecture sketched in Fig. 2 [20]. Note that the integration of the diagnostic residual generator $\boldsymbol{R}(z)\boldsymbol{r}_0(z)$ allows a reliable fault diagnosis and can be used, for instance, for the purpose of activating online updating of the control modules once a fault is detected.

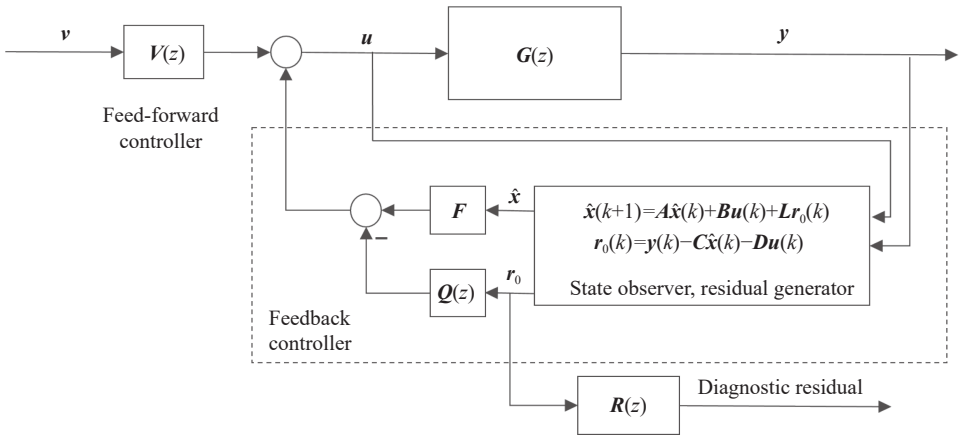

Fig. 2 An FTC architecture

Suppose that the control loop shown in Fig. 1 with the (nominal) controller

$$\boldsymbol{u}(z)=\boldsymbol{K}_0(z)\boldsymbol{y}(z)+\boldsymbol{v}(z)$$

is running stable but with degraded control performance. Since this controller can be equivalently written as

$$\boldsymbol{u}(z)=\boldsymbol{F}\boldsymbol{x}(z)-\boldsymbol{Q}_0(z)\boldsymbol{r}_0(z)+\bar{\boldsymbol{v}}(z)$$

for some $\boldsymbol{F}$ ensuring $\boldsymbol{A}+\boldsymbol{BF}$ being Schur and $\boldsymbol{Q}_0(z)\in\mathcal{RH}_\infty$, it follows from the observer-based realisation of Youla parameterisation that $\forall \boldsymbol{Q}(z)\in\mathcal{RH}_\infty$,

$$\begin{aligned}\boldsymbol{u}(z)=\boldsymbol{F}\boldsymbol{x}(z)-\boldsymbol{Q}_0(z)\boldsymbol{r}_0(z)+\bar{\boldsymbol{v}}(z)+\boldsymbol{Q}(z)\boldsymbol{r}_0(z)=\\ \boldsymbol{K}_0(z)\boldsymbol{y}(z)+\boldsymbol{v}(z)+\boldsymbol{Q}(z)\boldsymbol{r}_0(z),\end{aligned}\tag{46}$$

and thus the closed-loop dynamics with the new controller satisfying (46) is guaranteed stable. In fact, switching on or off the dynamic system $\boldsymbol{Qr}_0$ does not affect the system stability, when the switching rate is lower so that the switching effect can be neglected. Remember that feeding back the residual signal could enhance the system robustness and control performance, as will be demonstrated in our subsequent study as well. In this context, we call the configuration described by (46) and schematically sketched in Fig. 3 plug-and-play (PnP) FTC [21]. The most important feature of the PnP configuration consists in the realisation of FTC without any modification on the nominal controller $\boldsymbol{K}_0(z)$. This is of considerable practical interest in real applications.

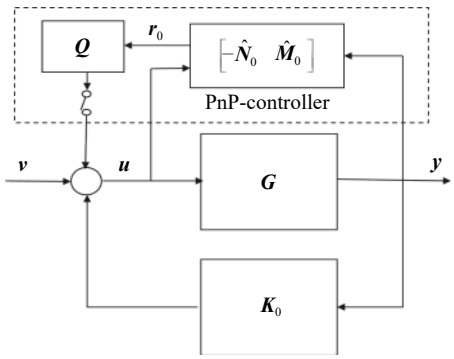

Fig. 3 PnP configuration of FTC

On the basis of the claim that the control signal $\boldsymbol{u}(k)$ is an estimate for $\boldsymbol{Fx}(k)+\bar{\boldsymbol{v}}(k)$ (in the sense of (45)), a further variant of the Youla parameterisation can be realised. Construct a state estimator as follows:

$$\begin{cases}\bar{\boldsymbol{x}}(k+1)=\boldsymbol{A}_L\bar{\boldsymbol{x}}(k)+\boldsymbol{B}_L\boldsymbol{u}(k)+\boldsymbol{L}\boldsymbol{y}(k)\\ \boldsymbol{A}_L=\boldsymbol{A}-\boldsymbol{LC},\ \ \boldsymbol{B}_L=\boldsymbol{B}-\boldsymbol{LD}\end{cases},\tag{47}$$

$$\begin{cases}\hat{\boldsymbol{x}}(z)=\bar{\boldsymbol{x}}(z)+\boldsymbol{R}(z)\boldsymbol{r}_0(z)\\ \boldsymbol{r}_0(k)=\boldsymbol{y}(k)-\boldsymbol{C}\bar{\boldsymbol{x}}(k)-\boldsymbol{Du}(k)\end{cases},\tag{48}$$

where $\boldsymbol{R}(z)\boldsymbol{r}_0(z)$ is added to increase the degree of design freedom for some parameterisation matrix $\boldsymbol{R}(z)\in\mathcal{RH}_\infty$. Now, according to (9), setting

$$\boldsymbol{u}(k)=\boldsymbol{F}\hat{\boldsymbol{x}}(k)+\bar{\boldsymbol{v}}(k)\tag{49}$$

results in

$$\boldsymbol{X}_0(z)\boldsymbol{u}(z)=-\boldsymbol{Y}_0(z)\boldsymbol{y}(z)+\bar{\boldsymbol{v}}(z)+\boldsymbol{FR}(z)\boldsymbol{r}_0(z)$$

$$\Longrightarrow$$

$$\begin{gathered}\boldsymbol{u}(z)=\boldsymbol{K}(z)\boldsymbol{y}(z)+\boldsymbol{v}(z),\\ \bar{\boldsymbol{v}}(z)=\left(\boldsymbol{X}_0(z)-\boldsymbol{Q}(z)\hat{\boldsymbol{N}}(z)\right)\boldsymbol{v}(z),\\ \boldsymbol{K}(z)=-\left(\boldsymbol{X}_0(z)-\boldsymbol{Q}(z)\hat{\boldsymbol{N}}(z)\right)^{-1}\left(\boldsymbol{Y}_0(z)+\boldsymbol{Q}(z)\hat{\boldsymbol{M}}(z)\right),\\ \boldsymbol{Q}(z)=-\boldsymbol{FR}(z),\end{gathered}$$

which is equivalent to a Youla parameterisation output feedback controller.

$$\boldsymbol{X}_0(z)\boldsymbol{u}(z)=-\boldsymbol{Y}_0(z)\boldsymbol{y}(z)+\bar{\boldsymbol{v}}(z)+\boldsymbol{FR}(z)\boldsymbol{r}_0(z)$$

We would like to draw the reader's attention to the state estimator (47)−(48). The feedback of the residual signal $\boldsymbol{Rr}_0$ provides us with a higher degree of design freedom and thus could deliver better estimation and detection performance. For instance, system (47)−(48) can be viewed as a general form of disturbance observers. A realisation of the system configuration is sketched in Fig. 4.

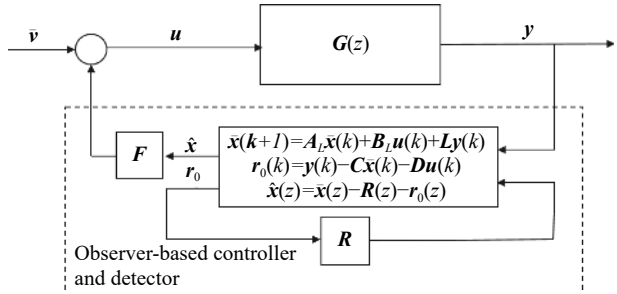

Fig. 4 Observer-based configuration with unified control and detection

2.4 Summary

As a summary of this section, we would like to underline the corner points of the control and detection unified framework. The information insight of feedback controllers, which has not received the deserved attention in research and practice, plays a central role in establishing and understanding the unified framework. We have demonstrated that a feedback controller is driven by the residual signal that is the information carrier about uncertainties in the control system under consideration. Moreover, a feedback controller is an estimator for the state feedback controller. These two (information) aspects unify control and detection functionalities.

While the integrated design of controller and fault detector in a control system is focused on controller and detector design based on a common design problem formulation [15], the control theoretical basis for the establishment of the unified framework is Youla parameterisation of all (LTI) stabilising controllers. The technical core of the unified framework is the observer-based realisation of Youla parameterisation. Based on it, modularisation and functionalisation of feedback controllers are achieved,

which, together with three variants of the system configuration, build the basis for the applications of the unified framework to detection, diagnosis and FTC in automatic control systems. To be specific, we are able to (i) gain deeper insight into intimate relations between control loop performance and fault detection, (ii) develop effective methods of detecting multiplicative faults in feedback control loops, (iii) detect system performance degradation, and (iv) recover the loop performance degradation (LPD). Some of these applications are reviewed and reported in the next section.

For our work, the factorisation technique is applied as the mathematical tool. The control theoretical interpretations of the LCF and RCF of plant dynamics and controllers are helpful to understand Youla parameterisation and Bezout identity that is very essential for the proof of Youla parameterisation.

3. Review of applications and new results

In this section, we review the reported applications of the control and detection unified framework to dealing with fault detection and FTC and associated modelling issues, and present some new results.

3.1 Residual centred system model

Consider the nominal system model (24) with the minimal state space realisation (2)−(3), the corresponding state observer and observer-based residual generator (10)−(12). Note that system (10)−(12) can be equivalently written as

$$\hat{\boldsymbol{x}}(k+1) = \boldsymbol{A}\hat{\boldsymbol{x}}(k) + \boldsymbol{B}\boldsymbol{u}(k) + \boldsymbol{L}\boldsymbol{r}_0(k), \tag{50}$$

$$\boldsymbol{y}(k) = \boldsymbol{r}_0(k) + \boldsymbol{C}\hat{\boldsymbol{x}}(k) + \boldsymbol{D}\boldsymbol{u}(k), \tag{51}$$

and its input-output dynamics is identical with one of (24). Moreover, for $\hat{\boldsymbol{x}}(0) = \boldsymbol{x}(0)$, $\hat{\boldsymbol{x}}(k) = \boldsymbol{x}(k), k = 1, 2, \cdots$ as well. That is, the dynamic system (50)−(51) is an alternative input-output (I/O)-model for the nominal system (24). In this regard, system model (50)−(51) is called observer-based I/O-model of (24).

Now, feedback control systems with the configuration shown in Fig. 1 are considered. Viewing the parameterisation form

$$\boldsymbol{u}(z) = \boldsymbol{F}\hat{\boldsymbol{x}}(z) - \boldsymbol{Q}(z)\boldsymbol{r}_0(z) + \bar{\boldsymbol{v}}(z) \tag{52}$$

where $\boldsymbol{Q}(z) \in \mathcal{RH}_\infty$, it is evident that all variables in the control system (52) are available in the observer-based I/O-model (50)−(51). This fact is of elemental importance for the subsequent work.

Next, the influences of uncertainties like unknown inputs, parameter variations and faults on the system dynamics are investigated. As mentioned before, we do not distinguish between disturbances and faults. Instead, summarise them as system uncertainties. For additive uncertainties represented by $\boldsymbol{d}$ and modelled by (25)−(26), the dynamics of $\boldsymbol{r}_0$ with respect to (w.r.t.) $\boldsymbol{d}$ is governed by

$$\begin{aligned} \boldsymbol{e}(k+1) &= (\boldsymbol{A} - \boldsymbol{L}\boldsymbol{C})\boldsymbol{e}(k) + (\boldsymbol{E}_d - \boldsymbol{L}\boldsymbol{F}_d)\boldsymbol{d}(k), \\ \boldsymbol{r}_0(k) &= \boldsymbol{C}\boldsymbol{e}(k) + \boldsymbol{F}_d\boldsymbol{d}(k), \\ \boldsymbol{e}(k) &= \boldsymbol{x}(k) - \hat{\boldsymbol{x}}(k). \end{aligned}$$

When, for instance, LCFU is under consideration,

$$\boldsymbol{y}(z) = \boldsymbol{G}(z)\boldsymbol{u}(z) = \left(\hat{\boldsymbol{M}}_0(z) + \boldsymbol{\Delta}_{\hat{M}}\right)^{-1}\left(\hat{\boldsymbol{N}}_0(z) + \boldsymbol{\Delta}_{\hat{N}}\right)u(z),$$

the dynamics of $\boldsymbol{r}_0$ w.r.t. $(\boldsymbol{\Delta}_{\hat{M}}, \boldsymbol{\Delta}_{\hat{N}})$ is described by

$$\boldsymbol{r}_0(z) = \boldsymbol{\Delta}_{\hat{N}}u(z) - \boldsymbol{\Delta}_{\hat{M}}\boldsymbol{y}(z). \tag{53}$$

It is noteworthy that all these types of uncertainties, not measurable and accessible, affect the model parameters and the dynamics of (24) as well as (2)−(3) directly. On the other hand, it is of considerable interest to notice that the configuration of observer-based I/O-model (50)−(51) is independent of the system uncertainties. Moreover, fully embedded in the residual vector $\boldsymbol{r}_0$, information about the uncertainties is accessible via the model (50)−(51). These two different model forms are schematically demonstrated in Fig. 5, in which $\boldsymbol{\Delta}$ indicates the system uncertainties schematically [21].

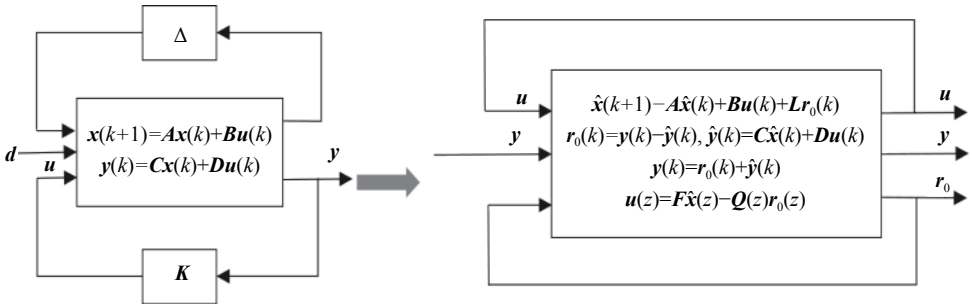

Fig. 5 From the standard model to the observer-based I/O-model: a schematic description

In summary, the residual centred closed-loop model is given at the end of this section,

$$\begin{aligned} \hat{\boldsymbol{x}}(k+1) &= \boldsymbol{A}\hat{\boldsymbol{x}}(k) + \boldsymbol{B}\boldsymbol{u}(k) + \boldsymbol{L}\boldsymbol{r}_0(k) = \\ &(\boldsymbol{A} + \boldsymbol{B}\boldsymbol{F})\hat{\boldsymbol{x}}(k) + \boldsymbol{B}\left(\boldsymbol{r}_{0,\boldsymbol{Q}}(k) + \bar{\boldsymbol{v}}(k)\right) + \boldsymbol{L}\boldsymbol{r}_0(k), \end{aligned} \tag{54}$$

$$\boldsymbol{x}_v(k+1)=(\boldsymbol{A}-\boldsymbol{LC})\boldsymbol{x}_v(k)+(\boldsymbol{B}-\boldsymbol{LC})\boldsymbol{v}(k), \tag{55}$$

$$\begin{aligned}\boldsymbol{y}(k)&=\boldsymbol{C}\hat{\boldsymbol{x}}(k)+\boldsymbol{D}\boldsymbol{u}(k)+\boldsymbol{r}_0(k)=\\&(\boldsymbol{C}+\boldsymbol{DF})\hat{\boldsymbol{x}}(k)+\boldsymbol{D}(\boldsymbol{r}_{0,\boldsymbol{Q}}(k)+\bar{\boldsymbol{v}}(k))+\boldsymbol{r}_0(k),\end{aligned} \tag{56}$$

$$\boldsymbol{u}(z)=\boldsymbol{F}\hat{\boldsymbol{x}}(z)-\boldsymbol{Q}(z)\boldsymbol{r}_0(z)+\bar{\boldsymbol{v}}(z) \tag{57}$$

$\Longrightarrow$

$$\begin{aligned}\boldsymbol{u}(k)&=\boldsymbol{F}\hat{\boldsymbol{x}}(k)+\boldsymbol{r}_{0,\boldsymbol{Q}}(k)+\bar{\boldsymbol{v}}(k),\\\boldsymbol{r}_0(k)&=\boldsymbol{y}(k)-\hat{\boldsymbol{y}}(k)=\\&\boldsymbol{y}(k)-(\boldsymbol{C}+\boldsymbol{DF})\hat{\boldsymbol{x}}(k)-\boldsymbol{D}(\boldsymbol{r}_{0,\boldsymbol{Q}}(k)+\bar{\boldsymbol{v}}(k)),\\\bar{\boldsymbol{v}}(z)&=\left(\boldsymbol{X}_0(z)-\boldsymbol{Q}(z)\hat{\boldsymbol{N}}(z)\right)\boldsymbol{v}(z)\end{aligned}$$

$\Longrightarrow$

$$\begin{aligned}\bar{\boldsymbol{v}}(k)&=\boldsymbol{v}(k)-\boldsymbol{F}\boldsymbol{x}_v(k)+\boldsymbol{v}_{\boldsymbol{Q}}(k),\\\boldsymbol{r}_{0,\boldsymbol{Q}}(z)&=-\boldsymbol{Q}(z)\boldsymbol{r}_0(z),\\\boldsymbol{v}_{\boldsymbol{Q}}(z)&=-\boldsymbol{Q}(z)\hat{\boldsymbol{N}}_0(z)\boldsymbol{v}(z)=-\boldsymbol{Q}(z)(\boldsymbol{D}+\boldsymbol{C}\boldsymbol{x}_v(z))\boldsymbol{v}(z).\end{aligned}$$

It is worth emphasising that $\boldsymbol{r}_0$ and $\boldsymbol{y}$ are signals with redundant information.

3.2 Diagnosis of additive faults and an FTC control scheme

Although additive faults do not affect the (closed-loop) system stability and eigen-dynamics, diagnosis and FTC schemes for this type of faults, due to their simple modelling form and intimate relations to many existing control theoretical problem formulations, attract most attention in research. In this section, we briefly review some solutions and their derivations based on the observer-based input-output model (50)−(51).

For our purpose, the uncertain model (25)−(26) is written as

$$\boldsymbol{x}(k+1)=\boldsymbol{A}\boldsymbol{x}(k)+\boldsymbol{B}\boldsymbol{u}(k)+\boldsymbol{\omega}(k)+\boldsymbol{E}_f\boldsymbol{f}(k), \tag{58}$$

$$\boldsymbol{y}(k)=\boldsymbol{C}\boldsymbol{x}(k)+\boldsymbol{D}\boldsymbol{u}(k)+\boldsymbol{\eta}(k)+\boldsymbol{F}_f\boldsymbol{f}(k) \tag{59}$$

where $\boldsymbol{\omega}(k)$ and $\boldsymbol{\eta}(k)$ are process and measurement noises, and $\boldsymbol{f}\in\mathbf{R}^{k_f}$ represents the (unknown) fault vector, which could be sensor and actuator faults and thus called hereafter system component faults. It is assumed that $\boldsymbol{\omega}(k)$ and $\boldsymbol{\eta}(k)$ are uncorrelated with the state and input vectors, and

$$\begin{aligned}\boldsymbol{\omega}(k)&\sim\mathcal{N}(\mathbf{0},\boldsymbol{\Sigma}_\omega),\\\boldsymbol{\eta}(k)&\sim\mathcal{N}\left(\mathbf{0},\boldsymbol{\Sigma}_\eta\right),\\\mathcal{E}\left(\begin{bmatrix}\boldsymbol{\omega}(i)\\\boldsymbol{\eta}(i)\\\boldsymbol{x}(0)\end{bmatrix}\begin{bmatrix}\boldsymbol{\omega}(j)\\\boldsymbol{\eta}(j)\\\boldsymbol{x}(0)\end{bmatrix}^{\mathrm{T}}\right)&=\begin{bmatrix}\begin{bmatrix}\boldsymbol{\Sigma}_\omega&\boldsymbol{S}_{\omega\eta}\\\boldsymbol{S}_{\omega\eta}^T&\boldsymbol{\Sigma}_\eta\end{bmatrix}\delta_{ij}&0\\0&\pi_0\end{bmatrix},\\\delta_{ij}&=\begin{cases}1,&i=j\\0,&i\neq j\end{cases}.\end{aligned}$$

Moreover, $\boldsymbol{E}_f,\boldsymbol{F}_f,\boldsymbol{\Sigma}_\omega,\boldsymbol{\Sigma}_\eta$, and $\boldsymbol{S}_{\omega\eta}$ are known matrices of appropriate dimensions.

It is well-known that the Kalman filter algorithm given below delivers a white residual vector $\boldsymbol{r}_0(k)$ with the minimum covariance matrix,

$$\begin{aligned}\hat{\boldsymbol{x}}(k+1)&=\boldsymbol{A}\hat{\boldsymbol{x}}(k)+\boldsymbol{B}\boldsymbol{u}(k)+\boldsymbol{L}_{\boldsymbol{K}}\boldsymbol{r}_0(k),\ \hat{\boldsymbol{x}}(0)=0,\\\boldsymbol{r}_0(k)&=\boldsymbol{y}(k)-\hat{\boldsymbol{y}}(k),\ \ \hat{\boldsymbol{y}}(k)=\boldsymbol{C}\hat{\boldsymbol{x}}(k)+\boldsymbol{D}\boldsymbol{u}(k),\\\boldsymbol{L}_{\boldsymbol{K}}&=\left(\boldsymbol{AYC}^{\mathrm{T}}+\boldsymbol{S}_{\omega\eta}\right)\boldsymbol{\Sigma}_r^{-1},\\\boldsymbol{Y}&=\boldsymbol{AYA}^{\mathrm{T}}+\boldsymbol{\Sigma}_\omega-\boldsymbol{L}_{\boldsymbol{K}}\boldsymbol{\Sigma}_r\boldsymbol{L}_{\boldsymbol{K}}^{\mathrm{T}},\\\boldsymbol{\Sigma}_r&=\mathcal{E}(\boldsymbol{r}_0(k)\boldsymbol{r}_0^{\mathrm{T}}(k))=\boldsymbol{CYC}^{\mathrm{T}}+\boldsymbol{\Sigma}_\eta.\end{aligned} \tag{60}$$

The whiteness of $\boldsymbol{r}_0$ allows us to approach the fault detection problem using the model

$$\boldsymbol{r}_0(k)=\boldsymbol{f}_r(k)+\boldsymbol{\varepsilon}(k),\ \boldsymbol{\varepsilon}(k)\sim\mathcal{N}(\mathbf{0},\boldsymbol{\Sigma}_r) \tag{61}$$

where $\boldsymbol{f}_r$ represents the influence of $\boldsymbol{f}$ on $\boldsymbol{r}_0$. Consequently, setting $\{J,J_{th}\}$ equal to

$$\begin{cases}J=\boldsymbol{r}_0^{\mathrm{T}}(k)\boldsymbol{\Sigma}_r^{-1}\boldsymbol{r}_0(k)\\J_{th}=\chi_\alpha^2\end{cases} \tag{62}$$

leads to an optimal fault detection, where α is the acceptable false alarm rate (FAR) [21].

It is the state of the art that, during fault-free operations, a linear quadratic Gaussian (LQG) controller delivers optimal control performance in the context of minimising the cost function of the following general form:

$$\begin{aligned}J(i)=\mathcal{E}\sum_{k=i}^{\infty}\gamma^{k-i}\begin{bmatrix}\boldsymbol{x}^{\mathrm{T}}(k)&\boldsymbol{u}^{\mathrm{T}}(k)\end{bmatrix}\begin{bmatrix}\boldsymbol{Q}_x&\boldsymbol{Q}_{xu}\\\boldsymbol{Q}_{ux}&\boldsymbol{Q}_u\end{bmatrix}\begin{bmatrix}\boldsymbol{x}(k)\\\boldsymbol{u}(k)\end{bmatrix},\\\begin{bmatrix}\boldsymbol{Q}_x&\boldsymbol{Q}_{xu}\\\boldsymbol{Q}_{ux}&\boldsymbol{Q}_u\end{bmatrix}\geqslant\mathbf{0},\ \boldsymbol{Q}_u>\mathbf{0},\\\boldsymbol{Q}_{ux}=\boldsymbol{Q}_{xu}^{\mathrm{T}},\ 0<\gamma<1.\end{aligned} \tag{63}$$

Without loss of generality, it is assumed that the (optimal) controller is Kalman filter based,

$$\boldsymbol{u}(k)=\boldsymbol{F}\hat{\boldsymbol{x}}(k),$$

with $\boldsymbol{v}=\mathbf{0}$. Although the solution to the LQG controller design is well-established, below we schematically illustrate the alternative solution based on the observer-based input-output model (50)−(51). Let

$$\min_{\boldsymbol{u}}J(i)=\hat{\boldsymbol{x}}^{\mathrm{T}}(i)\boldsymbol{X}\hat{\boldsymbol{x}}(i)+c$$

and following the dynamic programming method, write it as

$$\begin{aligned}\min_{\boldsymbol{u}}J(i)=\min_{\boldsymbol{u}(i)}\mathcal{E}\Big(&\begin{bmatrix}\boldsymbol{x}^{\mathrm{T}}(i)&\boldsymbol{u}^{\mathrm{T}}(i)\end{bmatrix}\begin{bmatrix}\boldsymbol{Q}_x&\boldsymbol{Q}_{xu}\\\boldsymbol{Q}_{ux}&\boldsymbol{Q}_u\end{bmatrix}\begin{bmatrix}\boldsymbol{x}(i)\\\boldsymbol{u}(i)\end{bmatrix}\\&[10pt]\gamma\hat{\boldsymbol{x}}^{\mathrm{T}}(i+1)\boldsymbol{X}\hat{\boldsymbol{x}}(i+1)+\gamma c\Big).\end{aligned}$$

Since $\boldsymbol{r}_0(k)$ is independent of $\hat{\boldsymbol{x}}(k)$ and $\boldsymbol{u}(k)$, and

$$\mathcal{E}(\boldsymbol{x}(k))=\hat{\boldsymbol{x}}(k),\mathcal{E}(\boldsymbol{r}_0(k))=\boldsymbol{0},$$
$$\mathcal{E}(\boldsymbol{x}^{\mathrm{T}}(k)\boldsymbol{Q}_x\boldsymbol{x}(k))=\mathcal{E}\boldsymbol{x}^{\mathrm{T}}(k)\boldsymbol{Q}_x\mathcal{E}\boldsymbol{x}(k)+\mathrm{tr}\left(\boldsymbol{Q}_x\mathcal{E}(\boldsymbol{x}(k)-\mathcal{E}\boldsymbol{x}(k))(\boldsymbol{x}(k)-\mathcal{E}\boldsymbol{x}(k))^{\mathrm{T}}\right)=\hat{\boldsymbol{x}}^{\mathrm{T}}(k)\boldsymbol{Q}_x\hat{\boldsymbol{x}}(k)+\mathrm{tr}(\boldsymbol{Q}_x\boldsymbol{Y}),$$
$$\boldsymbol{Y}=\mathcal{E}(\boldsymbol{x}(k)-\mathcal{E}\boldsymbol{x}(k))(\boldsymbol{x}(k)-\mathcal{E}\boldsymbol{x}(k))^{\mathrm{T}},$$
$$\mathcal{E}\left((\boldsymbol{L}_K\boldsymbol{r}_0(k))^{\mathrm{T}}\boldsymbol{X}\boldsymbol{L}_K\boldsymbol{r}_0(k)\right)=\mathrm{tr}(\boldsymbol{X}\boldsymbol{L}_K\boldsymbol{\Sigma}_r\boldsymbol{L}_K^{\mathrm{T}}),$$

it yields

$$\min_{\boldsymbol{u}(i)}J(i)=\min_{\boldsymbol{u}(i)}\left(\begin{bmatrix}\hat{\boldsymbol{x}}^{\mathrm{T}}(i) & \boldsymbol{u}^{\mathrm{T}}(i)\end{bmatrix}\boldsymbol{Q}\begin{bmatrix}\hat{\boldsymbol{x}}(i)\\ \boldsymbol{u}(i)\end{bmatrix}\right)+\mathrm{tr}(\boldsymbol{Q}_x\boldsymbol{Y})+\gamma\mathrm{tr}(\boldsymbol{X}\boldsymbol{L}\boldsymbol{\Sigma}_r\boldsymbol{L}^{\mathrm{T}})+\gamma c,$$
$$\boldsymbol{Q}=\begin{bmatrix}\boldsymbol{Q}_x+\gamma\boldsymbol{A}^{\mathrm{T}}\boldsymbol{X}\boldsymbol{A} & \boldsymbol{Q}_{xu}+\gamma\boldsymbol{A}^{\mathrm{T}}\boldsymbol{X}\boldsymbol{B}\\ \boldsymbol{Q}_{ux}+\gamma\boldsymbol{B}^{\mathrm{T}}\boldsymbol{X}\boldsymbol{A} & \boldsymbol{Q}_u+\gamma\boldsymbol{B}^{\mathrm{T}}\boldsymbol{X}\boldsymbol{B}\end{bmatrix}.$$

As a result, we have the final solution

$$\min_{\boldsymbol{u}(i)}J(i)=\hat{\boldsymbol{x}}^{\mathrm{T}}(i)\boldsymbol{X}\hat{\boldsymbol{x}}(i)+c,$$
$$\boldsymbol{u}^*(i)=\arg\min_{\boldsymbol{u}(i)}J(i)=\boldsymbol{F}_0\hat{\boldsymbol{x}}(i),$$
$$\boldsymbol{F}_0=-\left(\boldsymbol{Q}_u+\gamma\boldsymbol{B}^{\mathrm{T}}\boldsymbol{X}\boldsymbol{B}\right)^{-1}\left(\boldsymbol{Q}_{ux}+\gamma\boldsymbol{B}^{\mathrm{T}}\boldsymbol{X}\boldsymbol{A}\right),\tag{64}$$

with $\boldsymbol{X}$ and c satisfying

$$\boldsymbol{X}=\gamma\boldsymbol{A}^{\mathrm{T}}\boldsymbol{X}\boldsymbol{A}+\boldsymbol{Q}_x-\boldsymbol{F}_0^{\mathrm{T}}(\boldsymbol{Q}_u+\gamma\boldsymbol{B}^{\mathrm{T}}\boldsymbol{X}\boldsymbol{B})\boldsymbol{F}_0,\boldsymbol{X}>0,$$
$$c=\gamma c+\mathrm{tr}(\boldsymbol{Q}_x\boldsymbol{Y})+\gamma\mathrm{tr}(\boldsymbol{X}\boldsymbol{L}\boldsymbol{\Sigma}_r\boldsymbol{L}^{\mathrm{T}})$$
$$\Longrightarrow$$
$$c=\frac{\mathrm{tr}(\boldsymbol{Q}_x\boldsymbol{Y})+\gamma\mathrm{tr}(\boldsymbol{X}\boldsymbol{L}\boldsymbol{\Sigma}_r\boldsymbol{L}^{\mathrm{T}})}{1-\gamma}.$$

It is noteworthy that $\boldsymbol{F}_0$ in (64) is the linear quadratic feedback gain matrix. Moreover, recall the optimal estimate for the state vector delivered by the Kalman filter. It can be concluded that the optimal control is achieved by an optimal estimate of the optimal state feedback $\boldsymbol{F}_0\boldsymbol{x}(k)$.

Now, we consider an (optimal) FTC scheme in the case that the fault vector $\boldsymbol{f}(k)$ given in (58)−(59) is detected. The dynamics of the observer-based residual generator with respect to $\boldsymbol{f}$ is governed by

$$\boldsymbol{e}(k+1)=(\boldsymbol{A}-\boldsymbol{L}\boldsymbol{C})\boldsymbol{e}(k)+(\boldsymbol{E}_f-\boldsymbol{L}\boldsymbol{F}_f)\boldsymbol{f}(k),\tag{65}$$
$$\boldsymbol{r}_0(k)=\boldsymbol{C}\boldsymbol{e}(k)+\boldsymbol{F}_f\boldsymbol{f}(k).\tag{66}$$

It is well-known that with the observer gain matrix

$$\boldsymbol{L}=\boldsymbol{L}_2=\left(\boldsymbol{A}\boldsymbol{Y}\boldsymbol{C}^{\mathrm{T}}+\boldsymbol{E}_f\boldsymbol{F}_f^{\mathrm{T}}\right)\left(\boldsymbol{C}\boldsymbol{Y}\boldsymbol{C}^{\mathrm{T}}+\boldsymbol{F}_f\boldsymbol{F}_f^{\mathrm{T}}\right)^{-1},$$
$$\boldsymbol{Y}=\boldsymbol{A}\boldsymbol{Y}\boldsymbol{A}^{\mathrm{T}}+\boldsymbol{E}_f\boldsymbol{E}_f^{\mathrm{T}}-\boldsymbol{L}_2\left(\boldsymbol{C}\boldsymbol{Y}\boldsymbol{C}^{\mathrm{T}}+\boldsymbol{F}_f\boldsymbol{F}_f^{\mathrm{T}}\right)\boldsymbol{L}_2^{\mathrm{T}},$$

we have an $\mathcal{H}_2$ optimal observer [1]. Here, without loss of generality, it is assumed that $\boldsymbol{F}_f\boldsymbol{F}_f^{\mathrm{T}}=\boldsymbol{I}$. This motivates us to propose the following FTC scheme,

$$\begin{cases}\hat{\boldsymbol{x}}(k+1)=\boldsymbol{A}\hat{\boldsymbol{x}}(k)+\boldsymbol{B}\boldsymbol{u}(k)+\boldsymbol{L}\boldsymbol{r}_0(k)\\ \boldsymbol{u}(k)=\boldsymbol{F}_0\hat{\boldsymbol{x}}(k)\end{cases},$$
$$\boldsymbol{L}=\begin{cases}\boldsymbol{L}_K, \text{ fault-free}\\ \boldsymbol{L}_2, \text{ faulty}\end{cases}.\tag{67}$$

This fault-tolerant controller is of a simple and fixed configuration. In its core, it consists of a switching observer whose observer gain matrix is switched between the Kalman filter gain $\boldsymbol{L}_K$ and $\mathcal{H}_2$ optimal observer gain L_2. And, the switching is triggered by the fault detection logic.

Next, we would like to characterise the proposed detection and FTC system from the following system aspects, which are helpful to gain deeper insight into optimal fault detection and FTC.

(i) The observer (67) can serve as an estimator for the fault vector $\boldsymbol{f}(k)$, once the fault is detected and the observer is running with $\boldsymbol{L}=\boldsymbol{L}_2$.

Note that

$$\hat{\boldsymbol{f}}(k):=\boldsymbol{F}_f^{\mathrm{T}}\left(\boldsymbol{C}\boldsymbol{Y}\boldsymbol{C}^{\mathrm{T}}+\boldsymbol{F}_f\boldsymbol{F}_f^{\mathrm{T}}\right)^{-1}\boldsymbol{r}_0(k)\tag{68}$$

can be viewed as an estimate for the fault vector and the observer (67) is re-written as

$$\hat{\boldsymbol{x}}(k+1)=\boldsymbol{A}\hat{\boldsymbol{x}}(k)+\boldsymbol{B}\boldsymbol{u}(k)+\boldsymbol{L}_2\boldsymbol{r}_0(k)=$$
$$\boldsymbol{A}\hat{\boldsymbol{x}}(k)+\boldsymbol{B}\boldsymbol{u}(k)+\boldsymbol{E}_f\hat{\boldsymbol{f}}(k)+\boldsymbol{L}_x\boldsymbol{r}_0(k),$$
$$\boldsymbol{L}_x=\boldsymbol{A}\boldsymbol{Y}\boldsymbol{C}^{\mathrm{T}}\left(\boldsymbol{C}\boldsymbol{Y}\boldsymbol{C}^{\mathrm{T}}+\boldsymbol{F}_f\boldsymbol{F}_f^{\mathrm{T}}\right)^{-1}.$$

In [21,22], it is also called least squares (LS) estimate of the unknown input $\boldsymbol{f}(k)$.

(ii) On the assumption

$$\mathrm{rank}(\boldsymbol{G}_{yf}(z))=m,$$
$$\boldsymbol{G}_{yf}(z)=\boldsymbol{C}(z\boldsymbol{I}-\boldsymbol{A})^{-1}\boldsymbol{E}_f+\boldsymbol{F}_f,$$
$$\forall\theta\in[0,2\pi],\mathrm{rank}\begin{bmatrix}\boldsymbol{A}-\mathrm{e}^{\mathrm{j}\theta}\boldsymbol{I} & \boldsymbol{E}_d\\ \boldsymbol{C} & \boldsymbol{F}_d\end{bmatrix}=n+m,$$

the residual generator (65)−(66) connected with a post-filter

$$\boldsymbol{V}_r=\left(\boldsymbol{C}\boldsymbol{Y}\boldsymbol{C}^{\mathrm{T}}+\boldsymbol{F}_f\boldsymbol{F}_f^{\mathrm{T}}\right)^{-\frac{1}{2}}$$

is indeed a so-called co-inner system [1], i.e.,

$$\boldsymbol{r}(z):=\boldsymbol{V}_r\boldsymbol{r}_0(z)=\boldsymbol{V}_r\hat{\boldsymbol{N}}_f(z)\boldsymbol{f}(z),\tag{69}$$
$$\forall\theta\in[0,2\pi],\boldsymbol{V}_r\hat{\boldsymbol{N}}_f(\mathrm{e}^{\mathrm{j}\theta})\left(\boldsymbol{V}_r\hat{\boldsymbol{N}}_f(\mathrm{e}^{-\mathrm{j}\theta})\right)^{\mathrm{T}}=\boldsymbol{I},\tag{70}$$

$$\hat{\boldsymbol{N}}_f(z)=\boldsymbol{F}_f+\boldsymbol{C}(z\boldsymbol{I}-\boldsymbol{A}+\boldsymbol{L}_2\boldsymbol{C})^{-1}(\boldsymbol{E}_f-\boldsymbol{L}_2\boldsymbol{F}_f).$$

Consequently, it holds that

$$\|\boldsymbol{r}(z)\|_2 \leqslant \|\boldsymbol{f}(z)\|_2,\ \|\boldsymbol{r}(z)\|_2 = \|\boldsymbol{f}(z)\|_2,\ m = k_f.$$

Hence, the residual signal $\boldsymbol{r}(k)$ delivers an optimal estimation of the energy level of the fault vector. It is worth remarking that there exists the following relationship between the LS estimate (68) and $\boldsymbol{r}(k)$:

$$\left\|\hat{\boldsymbol{f}}(z)\right\|_2 = \|\boldsymbol{r}(z)\|_{2,\boldsymbol{W}} = \left\|\boldsymbol{W}^{\frac{1}{2}}\boldsymbol{r}(z)\right\|_2 \leqslant \|\boldsymbol{r}(z)\|_2,$$

$$\boldsymbol{W}^{\frac{1}{2}} = \boldsymbol{F}_f^{\mathrm{T}}\left(\boldsymbol{C}\boldsymbol{Y}\boldsymbol{C}^{\mathrm{T}} + \boldsymbol{F}_f\boldsymbol{F}_f^{\mathrm{T}}\right)^{-\frac{1}{2}} \Longrightarrow \sigma_{\max}\left(\boldsymbol{W}^{\frac{1}{2}}\right) \leqslant 1,$$

which demonstrates again that $\hat{\boldsymbol{f}}(k)$ is an estimate for $\boldsymbol{f}(k)$ satisfying the output equation

$$\boldsymbol{y}(k) = \boldsymbol{C}\boldsymbol{x}(k) + \boldsymbol{D}\boldsymbol{u}(k) + \boldsymbol{F}_f\boldsymbol{f}(k)$$

with the least l_2-norm.

(iii) It should be emphasised that, due to the existence of uncertainties in the system, e.g., noises or parameter variations, performing fault detection by means of the estimated fault, a very popular strategy as reported in the literature, leads to (very) poor detection performance. This can be evidently recognised by comparing the fault detection scheme with the test statistic and the threshold given in (62) and the use of the estimate $\hat{\boldsymbol{f}}(k)$ or $\boldsymbol{r}(k)$ for building the evaluation (detection) function.

(iv) In order to assess the influence of $\boldsymbol{f}(k)$ on the cost function $J(i)$ (63) under the use of the fault-tolerant controller (67), consider

$$\begin{bmatrix} \boldsymbol{x}^{\mathrm{T}}(k) & \boldsymbol{u}^{\mathrm{T}}(k) \end{bmatrix}\begin{bmatrix} \boldsymbol{Q}_x & \boldsymbol{Q}_{xu} \\ \boldsymbol{Q}_{ux} & \boldsymbol{Q}_u \end{bmatrix}\begin{bmatrix} \boldsymbol{x}(k) \\ \boldsymbol{u}(k) \end{bmatrix} =$$

$$\boldsymbol{x}^{\mathrm{T}}(k)\begin{bmatrix} \boldsymbol{I} & \boldsymbol{F}_0^{\mathrm{T}} \end{bmatrix}\begin{bmatrix} \boldsymbol{Q}_x & \boldsymbol{Q}_{xu} \\ \boldsymbol{Q}_{ux} & \boldsymbol{Q}_u \end{bmatrix}\begin{bmatrix} \boldsymbol{I} \\ \boldsymbol{F}_0 \end{bmatrix}\boldsymbol{x}(k) =: \boldsymbol{x}^{\mathrm{T}}(k)\boldsymbol{C}_z^{\mathrm{T}}\boldsymbol{C}_z x(k)$$

It holds that $\boldsymbol{C}_z\boldsymbol{x}(k) = \boldsymbol{C}_z\hat{\boldsymbol{x}}(k) + \boldsymbol{C}_z\boldsymbol{e}(k), \boldsymbol{e}(k) = \boldsymbol{x}(k) - \hat{\boldsymbol{x}}(k)$, whose frequency representation is given by

$$\boldsymbol{C}_z\boldsymbol{x}(z) = \boldsymbol{C}_z\Big((z\boldsymbol{I} - \boldsymbol{A} - \boldsymbol{B}\boldsymbol{F}_0)^{-1}\boldsymbol{L}_2\hat{\boldsymbol{N}}_f(z) + (z\boldsymbol{I} - \boldsymbol{A} + \boldsymbol{L}_2\boldsymbol{C})^{-1}(\boldsymbol{E}_f - \boldsymbol{L}_2\boldsymbol{F}_f)\Big)\boldsymbol{f}(z).$$

Remember that $\boldsymbol{V}_r\hat{\boldsymbol{N}}_f(z)$ is co-inner and hence $\left(\boldsymbol{V}_r\hat{\boldsymbol{N}}_f(z^{-1})\right)^{\mathrm{T}}$ is anti-stable, which yields

$$\begin{gathered}\left\|\boldsymbol{C}_z\left((z\boldsymbol{I} - \boldsymbol{A} - \boldsymbol{B}\boldsymbol{F}_0)^{-1}\boldsymbol{L}_2\hat{\boldsymbol{N}}_f(z) + (z\boldsymbol{I} - \boldsymbol{A} + \boldsymbol{L}_2\boldsymbol{C})^{-1}(\boldsymbol{E}_f - \boldsymbol{L}_2\boldsymbol{F}_f)\right)\right\|_2 = \\ \left\|\boldsymbol{C}_z\left((z\boldsymbol{I} - \boldsymbol{A} - \boldsymbol{B}\boldsymbol{F}_0)^{-1}\boldsymbol{L}_2\boldsymbol{V}_r^{-1} + (z\boldsymbol{I} - \boldsymbol{A} + \boldsymbol{L}_2\boldsymbol{C})^{-1}(\boldsymbol{E}_f - \boldsymbol{L}_2\boldsymbol{F}_f)\left(\boldsymbol{V}_r\hat{\boldsymbol{N}}_f(z^{-1})\right)^{\mathrm{T}}\right)\right\|_2 = \\ \left\|\boldsymbol{C}_z(z\boldsymbol{I} - \boldsymbol{A} - \boldsymbol{B}\boldsymbol{F}_0)^{-1}\boldsymbol{L}_2\boldsymbol{V}_r^{-1}\right\|_2 + \left\|\boldsymbol{C}_z(z\boldsymbol{I} - \boldsymbol{A} + \boldsymbol{L}_2\boldsymbol{C})^{-1}(\boldsymbol{E}_f - \boldsymbol{L}_2\boldsymbol{F}_f)\right\|_2,\end{gathered}$$

i.e., the $\mathcal{H}_2$-norm of the transfer function from $\boldsymbol{f}$ to $\boldsymbol{C}_z\boldsymbol{x}$ is minimum. In this sense, the proposed fault-tolerant controller minimises the influence of the detected fault on the control performance.

3.3 Detection of multiplicative faults and FTC schemes

3.3.1 Residual dynamics

Next, we consider the standard feedback control configuration sketched in Fig. 1 with plant model $\boldsymbol{G}$, feedback controller $\boldsymbol{K}$, and reference $\boldsymbol{v}$. We assume that

$$\boldsymbol{G}(z) = \hat{\boldsymbol{M}}^{-1}(z)\hat{\boldsymbol{N}}(z) = \boldsymbol{N}(z)\boldsymbol{M}^{-1}(z)$$

is corrupted either with the LCFU (35) or RCFU (36), and when

$$\text{for some given } \delta_{\mathcal{K}} > 0, \left\|\begin{bmatrix} -\boldsymbol{\Delta}_{\hat{N}} & \boldsymbol{\Delta}_{\hat{M}} \end{bmatrix}\right\|_\infty \leqslant \delta_{\mathcal{K}},$$

$$\text{or for some given } \delta_{\mathcal{I}} > 0, \left\|\begin{bmatrix} \boldsymbol{\Delta}_N \\ \boldsymbol{\Delta}_M \end{bmatrix}\right\|_\infty \leqslant \delta_{\mathcal{I}},$$

LCFU or RCFU represents (tolerable) model uncertainty. As the degradation becomes stronger,

$$\delta_{\mathcal{K}} < \left\|\begin{bmatrix} -\boldsymbol{\Delta}_{\hat{N}} & \boldsymbol{\Delta}_{\hat{M}} \end{bmatrix}\right\|_\infty \text{ or } \delta_{\mathcal{I}} < \left\|\begin{bmatrix} \boldsymbol{\Delta}_N \\ \boldsymbol{\Delta}_M \end{bmatrix}\right\|_\infty,$$

the uncertainty is defined as the fault to be detected.

Remark Hereafter, the domain operator z or k may be dropped out, when there is no risk of confusion.

Denoting all stabilisation controllers by

$$\boldsymbol{K}(z) = -\boldsymbol{U}(z)\boldsymbol{V}^{-1}(z) = -\hat{\boldsymbol{V}}^{-1}(z)\hat{\boldsymbol{U}}(z),$$

$$\begin{bmatrix} \hat{\boldsymbol{V}} & \hat{\boldsymbol{U}} \end{bmatrix} = \begin{bmatrix} \boldsymbol{X}_0 - \boldsymbol{Q}\hat{\boldsymbol{N}}_0 & \boldsymbol{Y}_0 + \boldsymbol{Q}\hat{\boldsymbol{M}}_0 \end{bmatrix},$$

$$\begin{bmatrix} \boldsymbol{U} \\ \boldsymbol{V} \end{bmatrix} = \begin{bmatrix} \hat{\boldsymbol{Y}}_0 + \boldsymbol{M}_0\boldsymbol{Q} \\ \hat{\boldsymbol{X}}_0 - \boldsymbol{N}_0\boldsymbol{Q} \end{bmatrix},$$

leads to the uncertainty-free closed-loop dynamics expressed in the following two (equivalent) forms:

$$\begin{gathered}\begin{bmatrix} \boldsymbol{u} \\ \boldsymbol{y} \end{bmatrix} = \begin{bmatrix} \boldsymbol{I} & -\boldsymbol{K} \\ -\boldsymbol{G} & \boldsymbol{I} \end{bmatrix}^{-1}\begin{bmatrix} \boldsymbol{I} \\ \boldsymbol{0} \end{bmatrix}\boldsymbol{v} = \\ \begin{bmatrix} \hat{\boldsymbol{V}} & \hat{\boldsymbol{U}} \\ -\hat{\boldsymbol{N}}_0 & \hat{\boldsymbol{M}}_0 \end{bmatrix}^{-1}\begin{bmatrix} \hat{\boldsymbol{V}} \\ \boldsymbol{0} \end{bmatrix}\boldsymbol{v} = \\ \begin{bmatrix} \boldsymbol{M}_0 & -\boldsymbol{U} \\ \boldsymbol{N}_0 & \boldsymbol{V} \end{bmatrix}\begin{bmatrix} \hat{\boldsymbol{V}} \\ \boldsymbol{0} \end{bmatrix}\boldsymbol{v} = \begin{bmatrix} \boldsymbol{M}_0 \\ \boldsymbol{N}_0 \end{bmatrix}\hat{\boldsymbol{V}}\boldsymbol{v} = \\ \begin{bmatrix} \boldsymbol{M}_0 & \boldsymbol{0} \\ \boldsymbol{0} & \boldsymbol{V} \end{bmatrix}\begin{bmatrix} \boldsymbol{M}_0 & \boldsymbol{U} \\ -\boldsymbol{N}_0 & \boldsymbol{V} \end{bmatrix}^{-1}\begin{bmatrix} \boldsymbol{I} \\ \boldsymbol{0} \end{bmatrix}\boldsymbol{v} = \begin{bmatrix} \boldsymbol{M}_0\hat{\boldsymbol{V}} \\ \boldsymbol{V}\hat{\boldsymbol{N}}_0 \end{bmatrix}\boldsymbol{v} = \\ \begin{bmatrix} \boldsymbol{I} \\ \boldsymbol{0} \end{bmatrix}\boldsymbol{v} + \begin{bmatrix} -\boldsymbol{U} \\ \boldsymbol{V} \end{bmatrix}\hat{\boldsymbol{N}}_0\boldsymbol{v}.\end{gathered} \tag{71}$$

In the above computations, the extended form of the Bezout identity (5),

$$\begin{bmatrix} \boldsymbol{M}_0 & -\boldsymbol{U} \\ \boldsymbol{N}_0 & \boldsymbol{V} \end{bmatrix}\begin{bmatrix} \hat{\boldsymbol{V}} & \hat{\boldsymbol{U}} \\ -\hat{\boldsymbol{N}}_0 & \hat{\boldsymbol{M}}_0 \end{bmatrix}=\begin{bmatrix} \boldsymbol{I} & \boldsymbol{0} \\ \boldsymbol{0} & \boldsymbol{I} \end{bmatrix},$$

is applied [21]. It is of interest to notice that relation (71) can also be applied to generating a residual vector as

$$\boldsymbol{r}_c := \begin{bmatrix} \boldsymbol{u} \\ \boldsymbol{y} \end{bmatrix} - \begin{bmatrix} \boldsymbol{M}_0 \\ \boldsymbol{N}_0 \end{bmatrix}\hat{\boldsymbol{V}}\boldsymbol{v}. \tag{72}$$

In fact, based on the residual centred closed-loop model (54)−(57), the above closed-loop residual generator can be derived as well. In our subsequent work, both residual vectors, $\boldsymbol{r}_0$ and $\boldsymbol{r}_c$, will be used for the detection purpose.

Under consideration of the LCFU (35), it holds that

$$\boldsymbol{r}_0 = \begin{bmatrix} \boldsymbol{\Delta}_{\hat{N}} & -\boldsymbol{\Delta}_{\hat{M}} \end{bmatrix}\begin{bmatrix} \boldsymbol{u} \\ \boldsymbol{y} \end{bmatrix} = \begin{bmatrix} \boldsymbol{\Delta}_{\hat{N}} & -\boldsymbol{\Delta}_{\hat{M}} \end{bmatrix}\begin{bmatrix} \hat{\boldsymbol{V}} & \hat{\boldsymbol{U}} \\ -\hat{\boldsymbol{N}}_0-\boldsymbol{\Delta}_{\hat{N}} & \hat{\boldsymbol{M}}_0+\boldsymbol{\Delta}_{\hat{M}} \end{bmatrix}^{-1}\begin{bmatrix} \hat{\boldsymbol{V}} \\ \boldsymbol{0} \end{bmatrix}\boldsymbol{v}.$$

Without loss of generality, it is assumed, in the above handling, that the same observer gain matrix $\boldsymbol{L}$ is shared by the residual generator and the LCF adopted in the controller. By Bezout identity, it is straightforward that

$$\begin{bmatrix} \hat{\boldsymbol{V}} & \hat{\boldsymbol{U}} \\ -\hat{\boldsymbol{N}}_0-\boldsymbol{\Delta}_{\hat{N}} & \hat{\boldsymbol{M}}_0+\boldsymbol{\Delta}_{\hat{M}} \end{bmatrix}^{-1}\begin{bmatrix} \hat{\boldsymbol{V}} \\ \boldsymbol{0} \end{bmatrix} = \left(\boldsymbol{I}+\begin{bmatrix} -\boldsymbol{U} \\ \boldsymbol{V} \end{bmatrix}\begin{bmatrix} -\boldsymbol{\Delta}_{\hat{N}} & \boldsymbol{\Delta}_{\hat{M}} \end{bmatrix}\right)^{-1}\begin{bmatrix} \boldsymbol{M}_0 \\ \boldsymbol{N}_0 \end{bmatrix}\hat{\boldsymbol{V}},$$

which further results in

$$\begin{aligned}\boldsymbol{r}_0 = {} & \begin{bmatrix} \boldsymbol{\Delta}_{\hat{N}} & -\boldsymbol{\Delta}_{\hat{M}} \end{bmatrix}\left(\boldsymbol{I}+\begin{bmatrix} -\boldsymbol{U} \\ \boldsymbol{V} \end{bmatrix}\begin{bmatrix} -\boldsymbol{\Delta}_{\hat{N}} & \boldsymbol{\Delta}_{\hat{M}} \end{bmatrix}\right)^{-1}\begin{bmatrix} \boldsymbol{M}_0 \\ \boldsymbol{N}_0 \end{bmatrix}\hat{\boldsymbol{V}}\boldsymbol{v} = \\ & -\left(\boldsymbol{I}+\begin{bmatrix} -\boldsymbol{\Delta}_{\hat{N}} & \boldsymbol{\Delta}_{\hat{M}} \end{bmatrix}\begin{bmatrix} -\boldsymbol{U} \\ \boldsymbol{V} \end{bmatrix}\right)^{-1}\begin{bmatrix} -\boldsymbol{\Delta}_{\hat{N}} & \boldsymbol{\Delta}_{\hat{M}} \end{bmatrix}\begin{bmatrix} \boldsymbol{M}_0 \\ \boldsymbol{N}_0 \end{bmatrix}\hat{\boldsymbol{V}}\boldsymbol{v}.\end{aligned} \tag{73}$$

Similarly, it holds that

$$\begin{aligned}\boldsymbol{r}_c &= \begin{bmatrix} \boldsymbol{u} \\ \boldsymbol{y} \end{bmatrix} - \begin{bmatrix} \boldsymbol{M}_0 \\ \boldsymbol{N}_0 \end{bmatrix}, \\ \hat{\boldsymbol{V}}\boldsymbol{v} &= \left(\left(\boldsymbol{I}+\begin{bmatrix} -\boldsymbol{U} \\ \boldsymbol{V} \end{bmatrix}\begin{bmatrix} -\boldsymbol{\Delta}_{\hat{N}} & \boldsymbol{\Delta}_{\hat{M}} \end{bmatrix}\right)^{-1}-\boldsymbol{I}\right)\begin{bmatrix} \boldsymbol{M}_0 \\ \boldsymbol{N}_0 \end{bmatrix}\hat{\boldsymbol{V}}\boldsymbol{v} = \\ & -\begin{bmatrix} -\boldsymbol{U} \\ \boldsymbol{V} \end{bmatrix}\begin{bmatrix} -\boldsymbol{\Delta}_{\hat{N}} & \boldsymbol{\Delta}_{\hat{M}} \end{bmatrix}\left(\boldsymbol{I}+\begin{bmatrix} -\boldsymbol{U} \\ \boldsymbol{V} \end{bmatrix}\begin{bmatrix} -\boldsymbol{\Delta}_{\hat{N}} & \boldsymbol{\Delta}_{\hat{M}} \end{bmatrix}\right)^{-1}\begin{bmatrix} \boldsymbol{M}_0 \\ \boldsymbol{N}_0 \end{bmatrix}\hat{\boldsymbol{V}}\boldsymbol{v} = \begin{bmatrix} -\boldsymbol{U} \\ \boldsymbol{V} \end{bmatrix}\boldsymbol{r}_0.\end{aligned}$$

It is worth noting that the relation between $\boldsymbol{r}_c$ and $\boldsymbol{r}_0$,

$$\boldsymbol{r}_c = \begin{bmatrix} -\boldsymbol{U} \\ \boldsymbol{V} \end{bmatrix}\boldsymbol{r}_0 \tag{74}$$

can be immediately found by the residual centered closed-loop model (54)−(57), which is indeed independent of the type of the uncertainty under consideration.

Next, we check the residual dynamics corresponding to the LCFU (36). It turns out that

$$\begin{aligned}\begin{bmatrix} \boldsymbol{u} \\ \boldsymbol{y} \end{bmatrix} &= \begin{bmatrix} \boldsymbol{I} & -\boldsymbol{K} \\ -\boldsymbol{G} & \boldsymbol{I} \end{bmatrix}^{-1}\begin{bmatrix} \boldsymbol{I} \\ \boldsymbol{0} \end{bmatrix}\boldsymbol{v} = \begin{bmatrix} \boldsymbol{M} & \boldsymbol{0} \\ \boldsymbol{0} & \boldsymbol{V} \end{bmatrix}\begin{bmatrix} \boldsymbol{M} & \boldsymbol{U} \\ -\boldsymbol{N} & \boldsymbol{V} \end{bmatrix}^{-1}\begin{bmatrix} \boldsymbol{I} \\ \boldsymbol{0} \end{bmatrix}\boldsymbol{v} = \\ & \begin{bmatrix} \boldsymbol{M} & \boldsymbol{0} \\ \boldsymbol{0} & -\boldsymbol{V} \end{bmatrix}\left(\boldsymbol{I}+\begin{bmatrix} \hat{\boldsymbol{V}} & \hat{\boldsymbol{U}} \end{bmatrix}\begin{bmatrix} \boldsymbol{\Delta}_M \\ \boldsymbol{\Delta}_N \end{bmatrix}\begin{bmatrix} \boldsymbol{0} & \boldsymbol{0} \\ \begin{bmatrix} -\hat{\boldsymbol{N}}_0 & \hat{\boldsymbol{M}}_0 \end{bmatrix}\begin{bmatrix} \boldsymbol{\Delta}_M \\ \boldsymbol{\Delta}_N \end{bmatrix} & \boldsymbol{I} \end{bmatrix}\right)^{-1}\begin{bmatrix} \hat{\boldsymbol{V}} \\ -\hat{\boldsymbol{N}}_0 \end{bmatrix}\boldsymbol{v} = \\ & \begin{bmatrix} \boldsymbol{M} & \boldsymbol{0} \\ \boldsymbol{0} & -\boldsymbol{V} \end{bmatrix}\begin{bmatrix} (\boldsymbol{I}+\boldsymbol{\Delta}_1)^{-1} & \boldsymbol{0} \\ -\boldsymbol{\Delta}_2(\boldsymbol{I}+\boldsymbol{\Delta}_1)^{-1} & \boldsymbol{I} \end{bmatrix}\begin{bmatrix} \hat{\boldsymbol{V}} \\ -\hat{\boldsymbol{N}}_0 \end{bmatrix}\boldsymbol{v},\end{aligned}$$

$$\boldsymbol{\Delta}_1 = \begin{bmatrix} \hat{\boldsymbol{V}} & \hat{\boldsymbol{U}} \end{bmatrix}\begin{bmatrix} \boldsymbol{\Delta}_M \\ \boldsymbol{\Delta}_N \end{bmatrix},\ \boldsymbol{\Delta}_2 = \begin{bmatrix} -\hat{\boldsymbol{N}}_0 & \hat{\boldsymbol{M}}_0 \end{bmatrix}\begin{bmatrix} \boldsymbol{\Delta}_M \\ \boldsymbol{\Delta}_N \end{bmatrix}.$$

Since

$$\begin{aligned}\boldsymbol{V}\boldsymbol{\Delta}_2(\boldsymbol{I}+\boldsymbol{\Delta}_1)^{-1}\hat{\boldsymbol{V}}+\boldsymbol{V}\hat{\boldsymbol{N}}_0 = {} & \\ \boldsymbol{N}_0\left(\boldsymbol{I}-\boldsymbol{\Delta}_1(\boldsymbol{I}+\boldsymbol{\Delta}_1)^{-1}\right)\hat{\boldsymbol{V}}+\boldsymbol{\Delta}_N(\boldsymbol{I}+\boldsymbol{\Delta}_1)^{-1}, & \\ \hat{\boldsymbol{V}} = \boldsymbol{N}(\boldsymbol{I}+\boldsymbol{\Delta}_1)^{-1}\hat{\boldsymbol{V}}, & \end{aligned} \tag{75}$$

we finally have

$$\begin{bmatrix} \boldsymbol{u} \\ \boldsymbol{y} \end{bmatrix} = \begin{bmatrix} \boldsymbol{M} \\ \boldsymbol{N} \end{bmatrix}(\boldsymbol{I}+\boldsymbol{\Delta}_1)^{-1}\bar{\boldsymbol{v}}. \tag{76}$$

Consequently, the dynamics of the residual generators are governed by

$$\begin{aligned}\boldsymbol{r}_0 &= \begin{bmatrix} -\hat{\boldsymbol{N}}_0 & \hat{\boldsymbol{M}}_0 \end{bmatrix}\begin{bmatrix} \boldsymbol{\Delta}_M \\ \boldsymbol{\Delta}_N \end{bmatrix}\left(\boldsymbol{I}+\begin{bmatrix} \hat{\boldsymbol{V}} & \hat{\boldsymbol{U}} \end{bmatrix}\begin{bmatrix} \boldsymbol{\Delta}_M \\ \boldsymbol{\Delta}_N \end{bmatrix}\right)^{-1}\bar{\boldsymbol{v}}, \\ \boldsymbol{r}_c &= \begin{bmatrix} -\boldsymbol{U} \\ \boldsymbol{V} \end{bmatrix}\boldsymbol{r}_0.\end{aligned} \tag{77}$$

Before we introduce the design of fault detection systems, we would like to call attention to the following facts:

(i) Comparing the residual dynamics (73) and (77) demonstrates clearly that the responses to the LCFU and

RCFU are in the dual form. For the simplicity, in the sequel, we only consider the RCFU case;

(ii) As far as the feedback control system is stable, the stability of the observer-based fault detection system is guaranteed. In addition, the control performance of the closed-loop expressed by $\left(\boldsymbol{I}+\begin{bmatrix}-\boldsymbol{\Delta}_{\hat{N}} & \boldsymbol{\Delta}_{\hat{M}}\end{bmatrix}\begin{bmatrix}-\boldsymbol{U}\\ \boldsymbol{V}\end{bmatrix}\right)^{-1}$ and $\left(\boldsymbol{I}+\begin{bmatrix}\hat{\boldsymbol{V}} & \hat{\boldsymbol{U}}\end{bmatrix}\begin{bmatrix}\boldsymbol{\Delta}_{\boldsymbol{M}}\\ \boldsymbol{\Delta}_{\boldsymbol{N}}\end{bmatrix}\right)^{-1}$ has influence on the dynamics of the fault detection system;

(iii) In the closed-loop configuration with RCFU, the corresponding "reference signal" for the RCF of the plant in the context of (18) is $(\boldsymbol{I}+\boldsymbol{\Delta}_1)^{-1}\bar{\boldsymbol{v}}$;

(iv) The residuals $\boldsymbol{r}_0$ and $\boldsymbol{r}_c$ can be viewed, from the information point of view, as being of the identical fault ability. For this reason, in our subsequent work, only $\boldsymbol{r}_0$ is applied for the detection and FTC purposes.

3.3.2 Design of the observer-based fault detection system

Concerning with the design of the observer-based fault detection system, threshold setting and the observer-based control system parameters should be determined. We first address the threshold setting issue on the assumptions:

(i) l_2-norm of the residual signal $\boldsymbol{r}_0$ is adopted for the detection purpose;

(ii) the threshold is determined based on the definition

$$J_{\text{th}}=\sup_{\left\|\begin{bmatrix}\boldsymbol{\Delta}_{\boldsymbol{M}} & \boldsymbol{\Delta}_{\boldsymbol{N}}\end{bmatrix}^{\mathrm{T}}\right\|_{\infty}\leqslant\delta_{\mathcal{I}},\bar{\boldsymbol{v}}\neq 0}\left(\frac{\|\boldsymbol{r}_0\|_2}{\|\bar{\boldsymbol{v}}\|_2}\right)\|\bar{\boldsymbol{v}}\|_2.$$

It follows from (77) that

$$\|\boldsymbol{r}_0\|_2=\left\|\begin{bmatrix}-\hat{\boldsymbol{N}}_0 & \hat{\boldsymbol{M}}_0\end{bmatrix}\begin{bmatrix}\boldsymbol{\Delta}_{\boldsymbol{M}}\\ \boldsymbol{\Delta}_{\boldsymbol{N}}\end{bmatrix}\left(\boldsymbol{I}+\begin{bmatrix}\hat{\boldsymbol{V}} & \hat{\boldsymbol{U}}\end{bmatrix}\begin{bmatrix}\boldsymbol{\Delta}_{\boldsymbol{M}}\\ \boldsymbol{\Delta}_{\boldsymbol{N}}\end{bmatrix}\right)^{-1}\bar{\boldsymbol{v}}\right\|_2\Longrightarrow$$

$$J_{\text{th}}=\sup_{\left\|\begin{bmatrix}\boldsymbol{\Delta}_{\boldsymbol{M}} & \boldsymbol{\Delta}_{\boldsymbol{N}}\end{bmatrix}^{\mathrm{T}}\right\|_{\infty}\leqslant\delta_{\mathcal{I}}}\left\|\begin{bmatrix}-\hat{\boldsymbol{N}}_0 & \hat{\boldsymbol{M}}_0\end{bmatrix}\begin{bmatrix}\boldsymbol{\Delta}_{\boldsymbol{M}}\\ \boldsymbol{\Delta}_{\boldsymbol{N}}\end{bmatrix}\left(\boldsymbol{I}+\begin{bmatrix}\hat{\boldsymbol{V}} & \hat{\boldsymbol{U}}\end{bmatrix}\begin{bmatrix}\boldsymbol{\Delta}_{\boldsymbol{M}}\\ \boldsymbol{\Delta}_{\boldsymbol{N}}\end{bmatrix}\right)^{-1}\right\|_{\infty}\|\bar{\boldsymbol{v}}\|_2.$$

Assume that

$$\forall\left\|\begin{bmatrix}\boldsymbol{\Delta}_{\boldsymbol{M}}\\ \boldsymbol{\Delta}_{\boldsymbol{N}}\end{bmatrix}\right\|_{\infty}\leqslant\delta_{\mathcal{I}},\left\|\begin{bmatrix}\hat{\boldsymbol{V}} & \hat{\boldsymbol{U}}\\ -\hat{\boldsymbol{N}}_0 & \hat{\boldsymbol{M}}_0\end{bmatrix}\begin{bmatrix}\boldsymbol{\Delta}_{\boldsymbol{M}}\\ \boldsymbol{\Delta}_{\boldsymbol{N}}\end{bmatrix}\right\|_{\infty}=\left\|\begin{bmatrix}\boldsymbol{\Delta}_1\\ \boldsymbol{\Delta}_2\end{bmatrix}\right\|_{\infty}\leqslant b<1 \tag{78}$$

$\Longrightarrow$

$$\sup_{\left\|\begin{bmatrix}\boldsymbol{\Delta}_{\boldsymbol{M}} & \boldsymbol{\Delta}_{\boldsymbol{N}}\end{bmatrix}^{\mathrm{T}}\right\|_{\infty}\leqslant\delta_{\mathcal{I}}}\left\|\begin{bmatrix}\hat{\boldsymbol{V}} & \hat{\boldsymbol{U}}\\ -\hat{\boldsymbol{N}}_0 & \hat{\boldsymbol{M}}_0\end{bmatrix}\begin{bmatrix}\boldsymbol{\Delta}_{\boldsymbol{M}}\\ \boldsymbol{\Delta}_{\boldsymbol{N}}\end{bmatrix}\right\|_{\infty}=\kappa_c\delta_{\mathcal{I}}=b, \tag{79}$$

$$\kappa_c:=\left\|\begin{bmatrix}\hat{\boldsymbol{V}} & \hat{\boldsymbol{U}}\\ -\hat{\boldsymbol{N}}_0 & \hat{\boldsymbol{M}}_0\end{bmatrix}\right\|_{\infty}. \tag{80}$$

It is a known result [23,24] that

$$\left\|\boldsymbol{\Delta}_2(\boldsymbol{I}+\boldsymbol{\Delta}_1)^{-1}\right\|_{\infty}\leqslant\frac{b}{\sqrt{1-b^2}}. \tag{81}$$

Thus,

$$J_{\text{th}}=\frac{b}{\sqrt{1-b^2}}\|\bar{\boldsymbol{v}}\|_2=\frac{\kappa_c\delta_{\mathcal{I}}}{\sqrt{1-(\kappa_c\delta_{\mathcal{I}})^2}}\|\bar{\boldsymbol{v}}\|_2. \tag{82}$$

We would like to mention that the condition (78) is, according to the small gain theorem, a sufficient condition so that the closed-loop is stable.

We now briefly discuss about the detection system design towards maximising the fault detectability in the unified framework of control and detection. It is state of the art in dealing with optimal fault detection that the detection (and control) system is designed in such a way that the residual is robust against uncertainties and simultaneously sensitivity to the faults to be detected as much as possible [1]. Considering that the threshold is an evaluation of the maximal influence of the uncertainty on the residual, the requirement on the robustness can be expressed as maximally reducing J_{th} so far allowed. For formulating the sensitivity handling, the minimum influence of the fault on the residual is checked according to

$$\inf_{\left\|\begin{bmatrix}\boldsymbol{\Delta}_{\boldsymbol{M}} & \boldsymbol{\Delta}_{\boldsymbol{N}}\end{bmatrix}^{\mathrm{T}}\right\|_{\infty}>\delta_{\mathcal{I}},\bar{\boldsymbol{v}}\neq 0}\left(\frac{\|\boldsymbol{r}_0\|_2}{\|\bar{\boldsymbol{v}}\|_2}\right)=\left\|\boldsymbol{\Delta}_2(\boldsymbol{I}+\boldsymbol{\Delta}_1)^{-1}\right\|_{-},$$

where $\left\|\boldsymbol{\Delta}_2(\boldsymbol{I}+\boldsymbol{\Delta}_1)^{-1}\right\|_{-}$ denotes the (nonzero) minimum singular value of $\boldsymbol{\Delta}_2(\boldsymbol{I}+\boldsymbol{\Delta}_1)^{-1}$, i.e.,

$$\min_{\theta}\sigma_{\min}\left(\boldsymbol{\Delta}_2(\boldsymbol{I}+\boldsymbol{\Delta}_1)^{-1}(\mathrm{e}^{\mathrm{j}\theta})\right).$$

Note that

$$\sigma_{\min}\left(\boldsymbol{\Delta}_2(\boldsymbol{I}+\boldsymbol{\Delta}_1)^{-1}(\mathrm{e}^{\mathrm{j}\theta})\right)\geqslant\sigma_{\min}\left(\boldsymbol{\Delta}_2(\mathrm{e}^{\mathrm{j}\theta})\right)\sigma_{\min}\left((\boldsymbol{I}+\boldsymbol{\Delta}_1)^{-1}(\mathrm{e}^{\mathrm{j}\theta})\right).$$

In summary, the design objective is

$$\begin{cases} \min \dfrac{\kappa_c \delta_{\bar{I}}}{\sqrt{1-(\kappa_c \delta_{\bar{I}})^2}} \\ \max \sigma_{\min}(\boldsymbol{\Delta}_2(\mathrm{e}^{\mathrm{j}\theta}))\,\sigma_{\min}\left((\boldsymbol{I}+\boldsymbol{\Delta}_1)^{-1}(\mathrm{e}^{\mathrm{j}\theta})\right) \end{cases}. \tag{83}$$

It is obvious that in (83) only the LCP of the controller, $(\hat{\boldsymbol{V}},\hat{\boldsymbol{U}})$, is the design parameter. Moreover, reducing $\left\|\begin{bmatrix}\hat{\boldsymbol{V}} & \hat{\boldsymbol{U}}\end{bmatrix}\right\|_\infty$ leads to the decrease of κ_c,

$$\kappa_c \leqslant \left\|\begin{bmatrix}\hat{\boldsymbol{V}} & \hat{\boldsymbol{U}}\end{bmatrix}\right\|_\infty + \left\|\begin{bmatrix}-\hat{\boldsymbol{N}}_0 & \hat{\boldsymbol{M}}_0\end{bmatrix}\right\|_\infty$$

and so $\dfrac{\kappa_c \delta_{\bar{I}}}{\sqrt{1-(\kappa_c \delta_{\bar{I}})^2}}$, as well as the increase of $\sigma_{\min}\left((\boldsymbol{I}+\boldsymbol{\Delta}_1)^{-1}(\mathrm{e}^{\mathrm{j}\theta})\right)$,

$$\sigma_{\min}\left((\boldsymbol{I}+\boldsymbol{\Delta}_1)^{-1}(\mathrm{e}^{\mathrm{j}\theta})\right) = \sigma_{\max}^{-1}\left((\boldsymbol{I}+\boldsymbol{\Delta}_1)(\mathrm{e}^{\mathrm{j}\theta})\right),$$

for smaller $\left\|\begin{bmatrix}\hat{\boldsymbol{V}} & \hat{\boldsymbol{U}}\end{bmatrix}\right\|_\infty$ implies larger $\sigma_{\max}((\boldsymbol{I}+\boldsymbol{\Delta}_1)(\mathrm{e}^{\mathrm{j}\theta}))$.

As a conclusion, minimising $\left\|\begin{bmatrix}\hat{\boldsymbol{V}} & \hat{\boldsymbol{U}}\end{bmatrix}\right\|_\infty$ subject to certain control performance requirements uniformly solves our optimal detection problem. We would like to emphasise that minimising $\left\|\begin{bmatrix}\hat{\boldsymbol{V}} & \hat{\boldsymbol{U}}\end{bmatrix}\right\|_\infty$ also increases the closed-loop stability margin and, as will be demonstrated in the next sub-section, improves the so-called loop recovery performance. Thanks to this nice property that unifies the tasks of (robust) controller design and optimal detection system design, we will not address the latter specifically and go directly over to FTC, which also performs an online optimisation of the controller and so leads to the improved fault detectability of the fault detection system. We would like to mention that an application of the proposed detection scheme to a case study on rolling mill processes as well as handling of fault isolation issues in the unified framework have been respectively reported in [25,26].

3.3.3 Stability margin monitoring and fault diagnosis

System stability is an essential requirement on any feedback controllers. In the sequel, a short analysis of stability degradation caused by $\boldsymbol{\Delta}_{\hat{\boldsymbol{M}}}$ and $\boldsymbol{\Delta}_{\hat{\boldsymbol{N}}}$ will be performed, and based on it, a fault diagnosis scheme towards stability margin monitoring will be introduced.

It is evident that $(\boldsymbol{\Delta}_{\hat{\boldsymbol{N}}},\boldsymbol{\Delta}_{\hat{\boldsymbol{M}}})$ affects the system stability, and, analogue to (78), the system is stable if

$$\left\|\begin{bmatrix}-\boldsymbol{\Delta}_{\hat{\boldsymbol{N}}} & \boldsymbol{\Delta}_{\hat{\boldsymbol{M}}}\end{bmatrix}\begin{bmatrix}\boldsymbol{M}_0 & -\boldsymbol{U}\\ \boldsymbol{N}_0 & \boldsymbol{V}\end{bmatrix}\right\|_\infty < 1.$$

For our purpose, we introduce the concept of fault-tolerant margin $b(\boldsymbol{K})$ as a function of the control law $\boldsymbol{K}$,

$$b(\boldsymbol{K}) = \left\|\begin{bmatrix}-\boldsymbol{\Delta}_{\hat{\boldsymbol{N}}} & \boldsymbol{\Delta}_{\hat{\boldsymbol{M}}}\end{bmatrix}\begin{bmatrix}\boldsymbol{M}_0 & -\boldsymbol{U}\\ \boldsymbol{N}_0 & \boldsymbol{V}\end{bmatrix}\right\|_\infty. \tag{84}$$

The fault-tolerant margin $b(\boldsymbol{K})$ is an indicator that characterises the performance degradation w.r.t. the stability caused by $(\boldsymbol{\Delta}_{\hat{\boldsymbol{M}}},\boldsymbol{\Delta}_{\hat{\boldsymbol{N}}})$. To be specific, a higher fault-tolerant margin is achieved by a smaller $b(\boldsymbol{K})$, and if $b(\boldsymbol{K})$ is approaching to one, the system is close to the stability margin. Hence, a good fault-tolerant controller should ensure $b(\boldsymbol{K}) < 1$. It is worth noting that $b(\boldsymbol{K})$ is closely related to the known stability margin concept in [23,27–29]. In fact, a lower $b(\boldsymbol{K})$ leads to a higher value of the loop stability margin. It is of remarkable practical interest to monitor the change of $b(\boldsymbol{K})$ online and to release an alarm timely as critical operations are approached. It is obvious that the fault detection scheme proposed in the previous sub-section cannot meet this requirement, since even for

$$\left\|\begin{bmatrix}-\boldsymbol{\Delta}_{\hat{\boldsymbol{N}}} & \boldsymbol{\Delta}_{\hat{\boldsymbol{M}}}\end{bmatrix}\right\|_\infty > \delta_{\mathcal{K}},$$

there exists no guarantee that

$$\|\boldsymbol{r}_0\|_2 = \left\|\left(\boldsymbol{I}+\begin{bmatrix}-\boldsymbol{\Delta}_{\hat{\boldsymbol{N}}} & \boldsymbol{\Delta}_{\hat{\boldsymbol{M}}}\end{bmatrix}\begin{bmatrix}-\boldsymbol{U}\\ \boldsymbol{V}\end{bmatrix}\right)^{-1}\begin{bmatrix}-\boldsymbol{\Delta}_{\hat{\boldsymbol{N}}} & \boldsymbol{\Delta}_{\hat{\boldsymbol{M}}}\end{bmatrix}\begin{bmatrix}\boldsymbol{M}_0\\ \boldsymbol{N}_0\end{bmatrix}\bar{\boldsymbol{v}}\right\|_2 > J_{th} \Longrightarrow \text{alarm}.$$

This demands for a specific monitoring scheme dedicated to monitoring $b(\boldsymbol{K})$. On the assumptions that the reference signal $\boldsymbol{v}$ satisfies the persistently excitation condition, and the measurements $\boldsymbol{u}(k)$ and $\boldsymbol{y}(k)$ are available, the following monitoring scheme based on the estimation of the lower bound of $b(\boldsymbol{K})$ can work efficiently. Let

$$\boldsymbol{r}_0(z) = \boldsymbol{P}_\Delta(z)\bar{\boldsymbol{v}}(z), \boldsymbol{P}_\Delta = -\left(\boldsymbol{I}+\begin{bmatrix}-\boldsymbol{\Delta}_{\hat{\boldsymbol{N}}} & \boldsymbol{\Delta}_{\hat{\boldsymbol{M}}}\end{bmatrix}\begin{bmatrix}-\boldsymbol{U}\\ \boldsymbol{V}\end{bmatrix}\right)^{-1}\begin{bmatrix}-\boldsymbol{\Delta}_{\hat{\boldsymbol{N}}} & \boldsymbol{\Delta}_{\hat{\boldsymbol{M}}}\end{bmatrix}\begin{bmatrix}\boldsymbol{M}_0\\ \boldsymbol{N}_0\end{bmatrix}.$$

According to the analogue form of (81) [24], it holds

$$\|\boldsymbol{P}_\Delta\|_\infty \leqslant \frac{b(\boldsymbol{K})}{\sqrt{1-b^2(\boldsymbol{K})}} \tag{85}$$

$$\Longleftrightarrow$$

$$b^2(\boldsymbol{K}) \geqslant \frac{\|\boldsymbol{P}_\Delta\|_\infty^2}{1+\|\boldsymbol{P}_\Delta\|_\infty^2}.$$

Thus, a lower bound of $b(\boldsymbol{K})$ can be estimated as long as $\|\boldsymbol{P}_\Delta\|_\infty$ is estimated by using the (online) available process data. To this end, the well-established algorithm of $\mathcal{H}_\infty$ norm estimation by using measurement data can be

applied [11]. For details, the reader is referred to [24].

In comparison with the existing fault detection methods, the advantages of the proposed approach mainly consists in data-driven and real-time detecting/estimating the fault-tolerant margin and indicating how far the stability margin is approached.

3.3.4 FTC schemes

Recall that $\boldsymbol{F},\boldsymbol{L}$, as high-priority parameters, and $\boldsymbol{Q}(z)$, as a low-priority parameter, are available in the residual centred FTC configuration for different functionalities. Below, we focus on designing and tuning the low-priority parameter $\boldsymbol{Q}$. To this end, we briefly introduce two schemes: (i) a passive FTC (P-FTC) scheme and (ii) an active FTC scheme (A-FTC).

The basic idea behind the P-FTC scheme is to reduce $b(\boldsymbol{K})$ based on the relation

$$b(\boldsymbol{K})=\left\|\begin{bmatrix}-\boldsymbol{\Delta}_{\hat{N}} & \boldsymbol{\Delta}_{\hat{M}}\end{bmatrix}\begin{bmatrix}\boldsymbol{M}_0 & -\hat{\boldsymbol{Y}}_0-\boldsymbol{M}_0\boldsymbol{Q}\\ \boldsymbol{N}_0 & \hat{\boldsymbol{X}}_0-\boldsymbol{N}_0\boldsymbol{Q}\end{bmatrix}\right\|_\infty$$

by solving

$$\boldsymbol{Q}^*=\arg\inf_{\boldsymbol{Q}\in\mathcal{RH}_\infty}\left\|\begin{bmatrix}\boldsymbol{M}_0 & -\hat{\boldsymbol{Y}}_0-\boldsymbol{M}_0\boldsymbol{Q}\\ \boldsymbol{N}_0 & \hat{\boldsymbol{X}}_0-\boldsymbol{N}_0\boldsymbol{Q}\end{bmatrix}\right\|_\infty, \tag{86}$$

when no additional constraint is to be satisfied. This is a model matching problem (MMP) and can be solved offline (design) by using the existing algorithms [30].

The A-FTC scheme consists of numerous steps and algorithms. If a fault alarm is released by the detection logic, $\boldsymbol{Q}\boldsymbol{r}_0$ is first plugged in to recover the stability margin by online reducing

$$\left\|\begin{bmatrix}\boldsymbol{M}_0 & -\hat{\boldsymbol{Y}}_0-\boldsymbol{M}_0\boldsymbol{Q}\\ \boldsymbol{N}_0 & \hat{\boldsymbol{X}}_0-\boldsymbol{N}_0\boldsymbol{Q}\end{bmatrix}\right\|_\infty$$

using the existing optimisation algorithms and without reconfiguring the operational controller [24]. Because it is not always in the situation that the degradation can be recovered by plugging in $\boldsymbol{Q}$, it can become necessary to reconfigure the operational controller to maintain the system performance. Considering the fault-tolerant issue in this light, the following performance degradation recovering (PDR) strategy is proposed: for a given threshold J_{th}, if $b(\boldsymbol{K})=:J(\boldsymbol{K})\geqslant J_{\text{th}}$, the controller $\boldsymbol{Q}(z)=\boldsymbol{Q}^*(z)$ is first implemented to accommodate the performance degradation. This action is labeled as PDR phase I. If for

$$\boldsymbol{K}^*=\begin{bmatrix}-\hat{\boldsymbol{Y}}_0-\boldsymbol{M}_0\boldsymbol{Q}^*\\ \hat{\boldsymbol{X}}_0-\boldsymbol{N}_0\boldsymbol{Q}^*\end{bmatrix},$$

it holds further $J(\boldsymbol{K}^*)\geqslant J_{\text{th}}$, the controller is re-constructed aiming at recovering the stability performance. This scheme is rated as PDR phase II.

In Fig. 6, the overall PDR strategy is illustrated schematically. For the detailed algorithms, we refer the reader to [24].

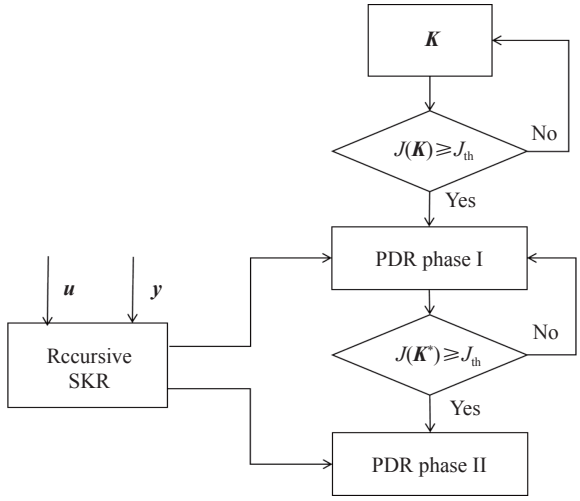

Fig. 6 Performance degradation recovering strategy

3.4 LPD monitoring and recovery

Loop transfer recovery (LTR) is a classic topic of control theory [11,31]. Roughly speaking, LTR deals with minimising the control performance loss caused by the use of an output feedback instead of a full state feedback. In this regard, LTR can be viewed as performance degradation recovery. This concept is extended to the assessment and monitoring of system performance degradation in a more general context.

3.4.1 LPD assessment and model

First, an ideal (reference) system performance model is defined. Consider (2)–(3) and write it as

$$\boldsymbol{x}_{\text{ideal}}(k+1)=\boldsymbol{A}\boldsymbol{x}_{\text{ideal}}(k)+\boldsymbol{B}\boldsymbol{u}_{\text{ideal}}(k), \tag{87}$$

$$\boldsymbol{y}_{\text{ideal}}(k)=\boldsymbol{C}\boldsymbol{x}_{\text{ideal}}(k)+\boldsymbol{D}\boldsymbol{u}_{\text{ideal}}(k). \tag{88}$$

Decoupled from any uncertainty, $\boldsymbol{x}_{\text{ideal}}(k)$ and $\boldsymbol{y}_{\text{ideal}}(k)$ denote the ideal state and output variables, respectively. Moreover,

$$\boldsymbol{u}_{\text{ideal}}(k):=\boldsymbol{F}\boldsymbol{x}_{\text{ideal}}(k)+\boldsymbol{v}(k) \tag{89}$$

is defined. In order to have a comparable basis for assessing the effect of use of an observer, it is assumed that either the reference signal $\boldsymbol{v}(k)$ given in (89) is generated by

$$\boldsymbol{v}(k)=\left(\boldsymbol{X}_0(z)-\boldsymbol{Q}(z)\hat{\boldsymbol{N}}_0(z)\right)\boldsymbol{v}_0(z)$$

or the output controller is realised in the observer-based form and the control signal is parameterised by

$$\boldsymbol{u}(z)=\boldsymbol{F}\hat{\boldsymbol{x}}(z)-\boldsymbol{Q}(z)\boldsymbol{r}_0(z)+\boldsymbol{v}(z).$$

Remember that $\boldsymbol{F}\hat{\boldsymbol{x}}(z)-\boldsymbol{Q}(z)\boldsymbol{r}_0(z)$ is an estimate for

$\boldsymbol{F}\boldsymbol{x}_{\text{ideal}}(z)$. Thus,

$$\boldsymbol{e}_{\boldsymbol{u}}(z)=\boldsymbol{u}_{\text{ideal}}(z)-\boldsymbol{u}(z)=\boldsymbol{F}\boldsymbol{e}_{\boldsymbol{x}}(z)+\boldsymbol{Q}(z)\boldsymbol{r}_0(z),\boldsymbol{e}_{\boldsymbol{x}}(z)=\boldsymbol{x}_{\text{ideal}}(z)-\hat{\boldsymbol{x}}(z),$$

specifies the (performance) loss in $\boldsymbol{u}$ due to the use of the estimate of $\boldsymbol{x}$. Similarly, let the difference

$$\boldsymbol{e}_{\boldsymbol{y}}(z)=\boldsymbol{y}_{\text{ideal}}(z)-\boldsymbol{y}(z)=\boldsymbol{y}_{\text{ideal}}(z)-\hat{\boldsymbol{y}}(z)-\boldsymbol{r}_0(z)=(\boldsymbol{C}+\boldsymbol{D}\boldsymbol{F})\boldsymbol{e}_{\boldsymbol{x}}(z)+\boldsymbol{D}\boldsymbol{Q}(z)\boldsymbol{r}_0(z)-\boldsymbol{r}_0(z)$$

indicate the loss in the output. Using the model (54)−(57) yields

$$\begin{aligned}\boldsymbol{e}_{\boldsymbol{x}}(z)&=(z\boldsymbol{I}-\boldsymbol{A}_{\boldsymbol{F}})^{-1}(\boldsymbol{B}\boldsymbol{Q}(z)-\boldsymbol{L})\boldsymbol{r}(z),\boldsymbol{A}_{\boldsymbol{F}}=\boldsymbol{A}+\boldsymbol{B}\boldsymbol{F},\\ \boldsymbol{e}_{\boldsymbol{u}}(z)&=\boldsymbol{F}(z\boldsymbol{I}-\boldsymbol{A}_{\boldsymbol{F}})^{-1}(\boldsymbol{B}\boldsymbol{Q}(z)-\boldsymbol{L})\boldsymbol{r}(z)+\boldsymbol{Q}(z)\boldsymbol{r}(z),\\ \boldsymbol{e}_{\boldsymbol{y}}(z)&=(\boldsymbol{C}+\boldsymbol{D}\boldsymbol{F})(z\boldsymbol{I}-\boldsymbol{A}_{\boldsymbol{F}})^{-1}(\boldsymbol{B}\boldsymbol{Q}(z)-\boldsymbol{L})\boldsymbol{r}(z)+\\ &\quad\ \boldsymbol{D}\boldsymbol{Q}(z)\boldsymbol{r}(z)-\boldsymbol{r}(z),\end{aligned}$$

which can be further written as

$$\boldsymbol{e}_{\text{LPD}}(z)=\begin{bmatrix}\boldsymbol{e}_{\boldsymbol{u}}(z)\\ \boldsymbol{e}_{\boldsymbol{y}}(z)\end{bmatrix}=\begin{bmatrix}\hat{\boldsymbol{Y}}_0(z)+\boldsymbol{M}_0(z)\boldsymbol{Q}(z)\\ -\hat{\boldsymbol{X}}_0(z)+\boldsymbol{N}_0(z)\boldsymbol{Q}(z)\end{bmatrix}\boldsymbol{r}_0(z).\quad(90)$$

System (90) is called LPD model (LPDM) with $\boldsymbol{r}_0$ and $\boldsymbol{e}_{\text{LPD}}$ as input and output, respectively. Correspondingly, $\boldsymbol{e}_{\text{LPD}}$ can be interpreted as the difference between the SIR of the ideal state feedback control case and the SIR of the real control system. As a result, tuning the controller directly reduces the (control) LPD.

3.4.2 Assessment and monitoring of control performance degradation

Now, $\boldsymbol{e}_{\text{LPD}}$ and LPDM (90) are adopted for the assessment of LPD. Suppose that the ideal system and $\boldsymbol{F}$ are given. As a reference system

$$\boldsymbol{x}(k+1)=\boldsymbol{A}\boldsymbol{x}(k)+\boldsymbol{B}u(k)+\boldsymbol{\omega}(k),\quad(91)$$

$$\boldsymbol{y}(k)=\boldsymbol{C}\boldsymbol{x}(k)+\boldsymbol{D}u(k)+\boldsymbol{\eta}(k)\quad(92)$$

is considered, where $\boldsymbol{\omega}(k)$ and $\boldsymbol{\eta}(k)$ are process and measurement noise vectors as described in (58)−(59). Corresponding to it, the (steady) Kalman filter (60) is assumed to be applied for generating the residual and estimating the state vector used in

$$\boldsymbol{u}(k)=\boldsymbol{F}\hat{\boldsymbol{x}}(k)+\boldsymbol{v}(k).\quad(93)$$

The state space model of LPDM (90) is

$$\boldsymbol{e}_{\boldsymbol{x}}(k+1)=(\boldsymbol{A}+\boldsymbol{B}\boldsymbol{F})\boldsymbol{e}_{\boldsymbol{x}}(k)-\boldsymbol{L}_{\boldsymbol{K}}\boldsymbol{r}_0(k),\quad(94)$$

$$\begin{cases}\boldsymbol{e}_{\boldsymbol{u}}(k)=\boldsymbol{F}\boldsymbol{e}_{\boldsymbol{x}}(k)\\ \boldsymbol{e}_{\boldsymbol{y}}(k)=(\boldsymbol{C}+\boldsymbol{D}\boldsymbol{F})\boldsymbol{e}_{\boldsymbol{x}}(k)-\boldsymbol{r}_0(k)\end{cases}.\quad(95)$$

We now introduce the following index as a reference for loop performance degradation assessment:

$$J_{\text{LPD},R}(i)=\mathcal{E}\sum_{k=i}^{\infty}\gamma^{k-i}\left(\boldsymbol{e}_{\boldsymbol{y}}^{\text{T}}(k)\boldsymbol{Q}_{\boldsymbol{y}}\boldsymbol{e}_{\boldsymbol{y}}(k)+\boldsymbol{e}_{\boldsymbol{u}}^{\text{T}}(k)\boldsymbol{Q}_{\boldsymbol{u}}\boldsymbol{e}_{\boldsymbol{u}}(k)\right),\ \boldsymbol{Q}_{\boldsymbol{y}}\geqslant\boldsymbol{0},\boldsymbol{Q}_{\boldsymbol{u}}\geqslant\boldsymbol{0},0<\gamma<1.\quad(96)$$

Straightforward computations lead to

$$J_{\text{LPD},R}(i)=\frac{\text{tr}(\boldsymbol{Q}\boldsymbol{\Sigma}_{\boldsymbol{e}_{\boldsymbol{x}}}+\boldsymbol{\Sigma}_{\boldsymbol{r}})}{1-\gamma},\quad(97)$$

$$\begin{aligned}\boldsymbol{Q}&=(\boldsymbol{C}+\boldsymbol{D}\boldsymbol{F})^{\text{T}}\boldsymbol{Q}_{\boldsymbol{y}}(\boldsymbol{C}+\boldsymbol{D}\boldsymbol{F})+\boldsymbol{F}^{\text{T}}\boldsymbol{Q}_{\boldsymbol{u}}\boldsymbol{F},\\ \boldsymbol{\Sigma}_{\boldsymbol{e}_{\boldsymbol{x}}}&=(\boldsymbol{A}+\boldsymbol{B}\boldsymbol{F})\boldsymbol{\Sigma}_{\boldsymbol{e}_{\boldsymbol{x}}}(\boldsymbol{A}+\boldsymbol{B}\boldsymbol{F})^{\text{T}}+\boldsymbol{L}_{\boldsymbol{K}}\boldsymbol{\Sigma}_{\boldsymbol{r}}\boldsymbol{L}_{\boldsymbol{K}}^{\text{T}}.\end{aligned}$$

Suppose that the dynamics of the real control system is described by the residual centred model (54)−(57) corrupted with uncertainties, including possible faults. Using the system models and measurement data, $\boldsymbol{r}_0(k),\hat{\boldsymbol{x}}(k),\boldsymbol{x}_{\text{ideal}}(k)$, $k=i,i+1,\cdots$, can be computed online and used to construct

$$\boldsymbol{\Sigma}_{\boldsymbol{e}_{\boldsymbol{x}}}=\frac{1}{N}\sum_{k=i}^{N+i}(\boldsymbol{x}_{\text{ideal}}(k)-\hat{\boldsymbol{x}}(k))(\boldsymbol{x}_{\text{ideal}}(k)-\hat{\boldsymbol{x}}(k))^{\text{T}},\quad\hat{\boldsymbol{\Sigma}}_{\boldsymbol{r}}=\frac{1}{N}\sum_{k=i}^{N+i}\boldsymbol{r}_0(k)\boldsymbol{r}_0^{\text{T}}(k).$$

The (online) performance degradation can then be estimated as

$$J_{\text{LPD}}(i)=\frac{\text{tr}\left(\boldsymbol{Q}\hat{\boldsymbol{\Sigma}}_{\boldsymbol{e}_{\boldsymbol{x}}}+\hat{\boldsymbol{\Sigma}}_{\boldsymbol{r}}\right)}{1-\gamma}.\quad(98)$$

Definition 1 Given $J_{\text{LPD},R}(i)$ and $J_{\text{LPD}}(i)$ defined in (97) and (98) respectively, the value

$$P_{LPD}(i)=1-\frac{J_{LPD,R}(i)}{J_{LPD}(i)}\quad(99)$$

is called the degree of LPD (DLPD) [21].

DLPD measures the difference between the ideal system input and output values and the real operating ones. When DLPD is larger than a given threshold, $P_{\text{LPD}}(i)>J_{th,\text{LPD}}$, an alarm is released that indicates unacceptable loop performance degradation.

3.4.3 LPD recovery

In the light of the LPDM (90), the LPD recovering issues can be dealt with in various ways. The first and also the easier way is to reduce the influence of the uncertainties (including faults), expressed in terms of the residual signal $\boldsymbol{r}_0$, on $\boldsymbol{e}_{\text{LPD}}$ that indicates the loop performance degradation. It follows from (90) that this can be achieved by minimising the norm of the transfer function matrix

$$\begin{bmatrix}\hat{\boldsymbol{Y}}_0(z)+\boldsymbol{M}_0(z)\boldsymbol{Q}(z)\\ -\hat{\boldsymbol{X}}_0(z)+\boldsymbol{N}_0(z)\boldsymbol{Q}(z)\end{bmatrix}$$

which is also the SIR of the controller. At this point, we call the reader's attention to the study in Section 3.3, in which we have revealed that reducing the $\mathcal{H}_\infty$ norm of

the controller SIR (as given above) (i) improves the system stability performance and (ii) enhances the fault detectability. In this context, we can now claim that reducing the $\mathcal{H}_\infty$ norm of the controller SIR unifiedly results in the increase of the loop stability margin, the increase of fault detectability and the enhancement of the ability of recovering LPD.

This is a fundamental result achieved in the unified framework of control and detection. An immediate application of this result is that the P-FTC and A-FTC schemes proposed in Section 3.3 can be fully adopted for the purpose of recovering performance degradation.

Recall that for $\boldsymbol{Q}=\boldsymbol{0}$, the LPDM (90) becomes

$$\boldsymbol{e}_{\boldsymbol{x}}(k+1)=(\boldsymbol{A}+\boldsymbol{BF})\boldsymbol{e}_{\boldsymbol{x}}(k)-\boldsymbol{L}\boldsymbol{r}_0(k), \tag{100}$$

$$\boldsymbol{e}_{\mathrm{LPD}}(k)=\begin{bmatrix}\boldsymbol{F}\\ \boldsymbol{C}+\boldsymbol{DF}\end{bmatrix}\boldsymbol{e}_{\boldsymbol{x}}(k)-\begin{bmatrix}\boldsymbol{0}\\ \boldsymbol{I}\end{bmatrix}\boldsymbol{r}_0(k). \tag{101}$$

It is evident that minimisation of the cost function

$$J_{\mathrm{LPD}}(i)=\sum_{k=i}^{\infty}\gamma^{k-i}\boldsymbol{e}_{\mathrm{LPD}}^{\mathrm{T}}(k)\boldsymbol{Q}_{\mathrm{LDP}}\boldsymbol{e}_{\mathrm{LPD}}(k),$$
$$\boldsymbol{Q}_{\mathrm{LDP}}\geqslant\boldsymbol{0},\ \ 0<\gamma<1,$$

with respect to $\boldsymbol{F},\boldsymbol{L}$, which leads to minimisation of the performance degradation, is in fact an $\mathcal{H}_2$ optimisation problem. In [21], a data-driven approach has been proposed to solve such an optimisation problem.

4. Future perspectives

In the previous section, we have illustrated and demonstrated that the proposed unified framework is helpful to gain deeper insight into intimate relations between control loop performance and fault detection, and can be efficiently applied for (i) detecting multiplicative faults in feedback control loops, (ii) detecting system performance degradation, and (iii) recovering the LPD. Some of the developed methods and algorithms have been successfully tested on real industrial and laboratory automatic control systems [19,32−35]. These achieved results have demonstrated that the proposed unified framework can be applied in major industrial sectors like automotive and process industries or in mechatronic and robotic systems and vision-based control systems.

In conclusion, we would like to introduce the following topics for the future research perspectives.

(i) Extensions of the unified framework to further classes of feedback control systems. The unified framework of control and detection introduced in this work has been established on the basis of Youla parameterisation for LTI systems. Recently, results of extending this work to singular and (general) nonlinear control systems have been reported [36,37]. It is expected that a further extension to time-varying systems would considerably expand the application domains of this framework. As demonstrated in some recent investigations, time-varying system models and the associated FDI methods can be, for instance, applied to dealing with FDI in switched systems and linear parameter varying (LPV) control systems [21] or event-triggered systems [38]. On the basis of such an extension, it is possible to study, for instance, fault and cyber-attack detection and diagnosis as well as performance degradation recovering issues in the unified framework for networked control systems and industrial cyber-physical systems. Our current works demonstrate the first promising results.

(ii) Data-driven realisation and implementation of the unified framework. In the era of industry 4.0 and big data, data-driven handling receives considerably increasing attention. Although our framework is based on system models and model-based controller and observer design, it is possible and realistic to implement this framework in the data-driven fashion. Such efforts are of significant practical interests. Remember that the theoretical basis of the framework is the LCF and RCF of dynamic systems (including both plant and controller under consideration). In some early works [20,39], the data-driven forms of LCF and RCF have been proposed and, based on them, applied for the FDI and FTC purposes [20,21,40], also for nonlinear systems [41]. This inspires and motivates data-driven realisation and implementation of the unified framework. In fact, a part of this framework has been adopted in the works reported in [21,40]. A further aspect of the data-driven realisation of the unified framework is that it enables an online optimisation of the control and (observer-based) detection system under consideration. This also establishes the basis for combining controller optimisation and machine learning methods towards online system optimisation by (data-driven) learning.

(iii) The unified framework based monitoring and recovering of system performance degradation. In the previous section, we have demonstrated that the proposed unified framework builds the fundament for monitoring and recovering of certain specified control system performance like stability margin or the LPD. FDI and FTC in the context of control performance degradation monitoring and recovering are attracting intensive attention in research and practical applications [32−35]. Some of the reported results have been inspired and supported by the algorithms and methods closely associated with the control and detection framework. We would like to call the reader's attention to the residual centered model (54)−(57) that provides us with an alternative possibility to model and deal with uncertainties including faults and hence allows us to assess the system performance and performance degradation efficiently. In fact, the application of the residual centred model (54)−(57) to LPD moni-

toring presented in the previous section demonstrates the potential of this effort. A successful application has been reported in [21].

A further application of the proposed unified framework is to approach predictive performance monitoring of feedback control systems, as reported in [21,33]. Prediction of control performance degradation is a basis for a reliable online control and control system optimisation as well as learning-based performance degradation recovering [21]. In this context, two major tasks are to be addressed, predictive detection of performance degradation and performance degradation prediction. This study could be, moreover, extended to predictive economic performance monitoring, in which not only the control performance but also some economic performance indicators could be included. This work would be of remarkable practical interests.

(iv) Multi-layer digital twin based predictive maintenance and product life-cycle management. In the recent decade, digital twin becomes a fashionable concept [42] and a powerful tool in many industrial sectors towards predictive maintenance and optimal production life-cycle management. In our previous work, a residual centred model has been introduced. It delivers sufficient information for feedback control, diagnosis, and performance monitoring. Based on the residual centred model, controllers, diagnostic and performance monitoring systems can be modularly built. For industrial applications, such a model should be of the ability of being adaptive to variations in system operating conditions and to uncertainties. In this context, we propose constructing a multi-layer digital twin for the life-cycle of an industrial automatic control system. The core of such a digital twin is the base layer consisting of the residual centred model that serves both as the process model and the system observer. In the second layer, control and diagnosis modules are integrated. In a further layer, the performance monitoring, prediction and recovery units are implemented. The learning and system optimisation algorithms are realised in the highest layer, which allow online updating of the residual centred model and control, diagnosis and performance prediction, monitoring and recovering modules to match varying operating conditions, variations due to uncertainties and even system component ageing. In Fig. 7, the structure of such a multi-layer digital twin is schematically sketched.

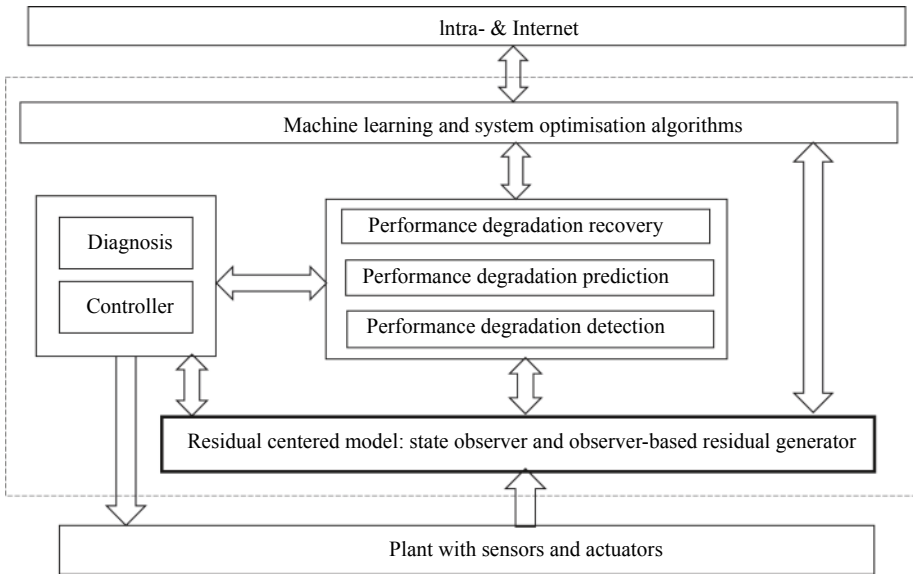

Fig. 7 Structure of a multi-layer digital twin

References

[1] DING S X. Model-based fault diagnosis techniques—design schemes, algorithms and tools. 2nd ed. London: Springer-Verlag, 2013.

[2] DU D S, JIANG B, SHI P, et al. Fault detection for continuous-time switched systems under asynchronous switching. International Journal of Robust and Nonlinear Control, 2014, 24(11): 1694–1704.

[3] SHEN Q S, JIANG B, SHI P. Fault diagnosis for T-S fuzzy systems with sensor faults and system performance analysis. IEEE Trans. on Fuzzy Systems, 2014, 22(2): 274–284.

[4] NETT C N, JACOBSON C, MILLER A T. An integrated approach to controls and diagnostics. Proc. of the American Control Conference, 1988: 824–835.

[5] JACOBSON C, NETT C. An integrated approach to controls and disgnostics using the four parameter controller. IEEE Control Systems Magazine, 1991, 11(6): 22–29.

[6] TYLER M L, MORARI M. Optimal and robust design of integrated control and diagnostic modules. Proc. of American Control Conference, 1994: 2060–2064.

[7] MURAD G, POSTLETHWAITE I, GU D W. A robust design approach to integrated control and diagnostics. Proc. of the 13th International Federation of Automatic Control Word Congress, 1996, 7: 199–204.

[8] KISGAARD S, RANK M, NIEMANN H, et al. Simulta-

neous design of controller and fault detector. Proc. of the 35th IEEE Conference on Decision and Control, 1996: 628–629.
[9] SOUTSTRUP J, GRIMBLE M, NIEMANN H. Design of integrated systems for the control and detection of actuator/sensor faults. Sensor Review, 1997, 17(2): 138–149.
[10] NIEMANN H, SOUTSTRUP J. Integration of control and fault detection: nominal and robust design. Proc. of the 3rd International Federation of Automatic Control Symposium, 1997, 30(18): 341–346.
[11] ZHOU K M, DOYLE J, GLOVER K. Robust and optimal control. New Jersey: Prentice-Hall, 1996.
[12] KHOSROWJERDI M J, NIKOUKHAH R, SAFARI-SHAD N. A mixed H-2/H-infinity approach to simultaneous fault detection and control. Automatica, 2004, 40(2): 261–267.
[13] WENG Z X, PATTON R, CUI P. Integrated design of robust controller and fault estimator for linear parameter varying systems. Proc. of the 17th International Federation of Automatic Control World Congress, 2008, 41(2): 4535–4539.
[14] WANG H, YANG G H. Integrated fault detection and control for LPV systems. International Journal of Robust and Nonlinear Control, 2009, 19(3): 341–363.
[15] DING S X. Integrated design of feedback controllers and fault detectors. Annual Reviews in Control, 2009, 33(2): 124–135.
[16] HENRY D, ZOLGHADRI A. Design and analysis of robust residual generators for systems under feedback control. Automatica, 2005, 41(2): 251–264.
[17] SUZUKI T, TOMIZUKA M. Joint synthesis of fault detector and controller based on structure of two-degree-of-freedom control system. Proc. of the 38th IEEE Conference on Decision and Control, 1999: 3599–3604.
[18] ZHOU K M, REN Z. A new controller architecture for high performance, robust, and fault-tolerant control. IEEE Trans. on Automatic Control, 2001, 46(10): 1613–1618.
[19] DING S X, YANG G J, ZHANG P, et al. Feedback control structures, embedded residual signals and feedback control schemes with an integrated residual access. IEEE Trans. on Control Systems Technology, 2010, 18(2): 352–367.
[20] DING S X. Data-driven design of fault diagnosis and fault-tolerant control systems. London: Springer-Verlag, 2014.
[21] STEVEN X D. Advanced methods for fault diagnosis and fault-tolerant control. Berlin: Springer-Verlag, 2020.
[22] WILLEMS J. Deterministic least squares filtering. Journal of Econometrics, 2014, 118(1/2): 341–373.
[23] GEORGIOU T T, SMITH M C. Optimal robustness in the gap metric. IEEE Trans. on on Automatic Control, 1990, 35(6): 673–686.
[24] LI L L, LUO H, DING S X. Performance-based fault detection and fault-tolerant control for automatic control systems. Automatica, 2019, 99: 308–316.
[25] DING S X, LI L L. Gap metric techniques and their application to fault detection performance analysis and fault isolation schemes. Automatica, 2020, 118: 109029.
[26] LI L L, DING S X. Optimal detection schemes for multiplicative faults in uncertain systems with application to rolling mill processes. IEEE Trans. on Control Systems Technology, 2020, 28(6): 2432–2444.
[27] VIDYASAGAR M, KIMURA H. Robust controllers for uncertain linear variable systems. Automatica, 1986, 22: 85–94.
[28] VINNICOMBE G. Uncertainty and feedback: H loop-shaping and the V-gap metric. Singapore: World Scientific, 2000.
[29] SKOGESTAD S, POSTLETHWAITE I. Multivariable feedback control. New York: John Wiley and Sons, Ltd, 2005.
[30] FRANCIS B A. A course in H-infinity control theory. Berlin/New York: Springer-Verlag, 1987.
[31] TAY T T, MAREELS I, MOORE J B. High performance control. New York: Springer Science & Business Media, 1998.
[32] LI L L, DING S X, LUO H, et al. Performance-based fault-tolerant control approaches for industrial processes with multiplicative faults. IEEE Trans. on Industrial Information, 2020, 16(7): 4759–4768.
[33] LI L L, DING S X. Performance supervised fault detection schemes for industrial feedback control systems and their data-driven implementation. IEEE Trans. on Industrial Information, 2020, 16(4): 2849–2858.
[34] LUO H, YIN S, LIU T Y, et al. A data-driven realization of the control performance-oriented process monitoring system. IEEE Trans. on Industrial Electronics, 2020, 67(1): 521–530.
[35] XU Y S, DING S X, LUO H, et al. A real-time performance recovery framework for vision-based control systems. IEEE Trans. on Industrial Electronics, 2021, 68(2): 1571–1580.
[36] LIU D, YANG Y, LI L L, et al. Control performance-based fault-tolerant control strategy for singular systems. IEEE Trans. on Systems, Man, and Cybernetics: Systems, 2020, 50(7): 2398–2407.
[37] HAN H Y, YANG Y, LI L L, et al. Performance-based fault detection and fault-tolerant control for nonlinear systems with T-S fuzzy implementation. IEEE Trans. on Cybernetics, 2021, 51(2): 801–804.
[38] ZHONG M Y, DING S X, ZHOU D H, et al. An H_i/H_∞ optimization approach to event triggered fault detection for linear discrete time systems. IEEE Trans. on Automatic Control, 2020, 65(10): 4464–4471.
[39] DING S X, YANG Y, ZHANG Y, et al. Data-driven realization of kernel and image representations and their application to fault detection and control system design. Automatica, 2014, 50(10): 2615–2623.
[40] YANG X, GAO J J, LUO H, et al. Data-driven design of fault tolerant control systems based on recursive stable image representation. Automatica, 2020, 122: 109246.
[41] LI L L, DING S X, YANG Y, et al. A fault detection approach for nonlinear systems based on data-driven realizations of fuzzy kernel representations. IEEE Trans. on Fuzzy Systems, 2018, 26(4): 1800–1812.
[42] GRIEVES M. Virtually intelligent product systems: digital and physical twins. Virginia: American Institute of Aeronautics and Astronautics, 2019.

Biographies

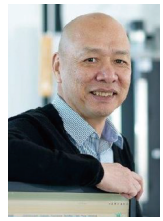

DING Steven Xianchuan was born in 1959. He received his Ph.D. degree in electrical engineering from the Gerhard-Mercator University of Duisburg, Germany, in 1992. From 1992 to 1994, he was a research and development engineer with Rheinmetall. From 1995 to 2001, he was a professor of control engineering with the University of Applied Science Lausitz, Senftenberg, Germany, where he served as a vice president from 1998 to 2000. Since 2001, he has been the chair professor of control engineering and head of the Institute for Automatic Control and Complex Systems with the University of Duisburg-Essen, Germany. His research interests are model-based and data-driven fault diagnosis, control and fault-tolerant systems, and their application in industry with a focus on automotive systems, chemical processes, and renewable energy systems.
E-mail: steven.ding@uni-due.de

LI Linlin was born in 1987. She received her B.E. degree from Xi 'an Jiaotong University, China, in 2008, M.E. degree from Peking University, China, in 2011, and Ph.D. degree from the Institute for Automatic Control and Complex Systems (AKS), University of Duisburg-Essen, Germany. She is currently an associate professor with the School of Automation and Electrical Engineering, University of Science and Technology Beijing, China. Her research interests include fault diagnosis and fault tolerant control, fuzzy control, and estimation for nonlinear systems.

E-mail: linlin.li@ustb.edu.cn

JIANG Bin was born in 1966. He received his Ph.D. degree in automatic control from Northeastern University, Shenyang, China, in 1995. He has been a postdoctoral fellow or a research fellow in Singapore, France, and the USA, and a visiting professor in Canada. He is currently a chair professor of Cheung Kong Scholar Program in Ministry of Education, and vice president in Nanjing University of Aeronautics and Astronautics, Nanjing, China. His current research interests include fault diagnosis and fault-tolerant control and their applications.

E-mail: binjiang@nuaa.edu.cn